JOURNAL OF GEOPHYSICAL RESEARCH, VOL. 106, NO. C11, PAGES 27,187–27,204, NOVEMBER 15, 2001

Deterministic Modelling of Driving and Dissipation for Ocean Surface Gravity Waves

Jorge F. Willemsen

Rosenstiel School of Marine and Atmospheric Science, University of Miami, Miami, Florida

Abstract. Consider two questions. What qualitative features should a spectrum of wind driven wave amplitudes possess in deep water? Then, is it possible to compute such a spectrum ab initio? In answer to the first question, at the least the spectrum should exhibit a spectral peak determined by the acting wind; an asymptotic power law tail; and an angular dependence between the dominant wind and wave directions. The principal result of this paper is that a model to calculate a wind-driven sea spectrum that satisfies the first two requirements starting from a broad suite of initial conditions has been constructed and exercised. To this end, wind driving mechanisms and models for dissipation caused by wave breaking are investigated. This study does not include detailed hydrodynamic calculations, but rather an evaluation of physically plausible model interaction terms. These are appended to Hamilton's equations for a wave field in deep water. This methodology leads to deterministic ordinary differential equations for the evolution of the wave field in which three and four wave nonlinear interactions are incorporated. The deterministic form of the equations is preserved through the introduction of nonstochastic driving and dissipation terms. The time evolution results presented fulfill the qualitative expectations desired for the spectrum. The calculations also yield much more information. Full phase information is retained. The relative magnitudes of the nonlinear interaction terms may be assessed as functions of time. The same applies for the magnitudes of the driving and dissipating terms. This information will be used to improve the model to where it is ready to confront experimental data.

1. Introduction

The objective of this paper is to introduce driving and dissipation terms into the Krasitskii (1994) formulation of Hamilton's Equations for ocean surface gravity waves in a manner that produces wave spectra in qualitative agreement with experiment. Remarkably there is little in the literature to indicate that the incorporation of such terms has been considered in a systematic fashion. Indeed examples of including dissipation within deterministic models are usually ad hoc, see e.g., *Smith* [1998] and *Watson and Buchsbaum* [1996]. The term ad hoc does not need to be taken in a perjorative sense: the terms used in these works were in accord with the stated aims of their investigations. Nonetheless it seems that a systematic examination of driving and dissipation within a deterministic framework is not only appropriate, but even overdue.

The viability of a fast Fourier transform (FFT) computational method for solving Krasitskii's equations, employing a convolution method for computing the nonlinear interaction terms, has been demonstrated in the absence of driving and dissipation [*Willemsen*, 1998]. The motivation for that work resided in part with a perceived need for rapid yet accurate calculation of the evolution of the sea state for use, for example, in navigation. By way of introduction it is useful to list the principal results of that paper. They are as follows: (1) the FFT formulation was succesfully implemented; (2) numerical stability was achieved, as evidenced by extremely accurate energy conservation; (3) rapid growth of modes in resonance with respect to others was exhibited; and (4) it took appxroximately 15 s of computer time to model 1 s of wave evolution using the convolution method and of the order of 10 times this doing straightforward numerical integrations. This time is not blazingly fast, but the work was performed on a circa 1992 machine. The calculations run much faster on a state of the art platform.

In a further development, the fully nonlinear evolution of an asymmetric Gaussian wave group has been investigated [*Willemsen*, 2001]. Such idealized waveforms are an excellent laboratory, both theoretically and experimentally, for investigating effects of nonlinearity on wave steepening and thus on the approach to wave breaking [*Magnusson et al.*, 1999; *Banner and Tian*, 1998]. An important result from this study stems from the observation that wave steepening may occur within the calculation as a consequence of interference between two or more waves. However, nonlinear dephasing of the spectral configuration which leads to steepening in x space can cause the high end of the spectrum to grow catastrophically. The precise manner in which this occurs was discussed and illustrated with examples by *Willemsen* [2001]. In brief, only the nonlinear interactions can "pump" excess energy from one part of the spectrum to another. Within the numerics the excessive growth manifests as an "ultraviolet" instability.

The above observation can be interpreted as a signal that a cutoff on the wave steepness should be imposed to prevent such catastrophic growth. Physically this would correspond to wave breaking when the wave steepness exceeds an appropriate threshold.

Thus the next logical step in the computational program is to incorporate driving and dissipation terms into the dynamical equa-

Paper number 2000JC000325.
0148-0227/01/2000JC000325$09.00

tions of motion. This will be done following a brief review of the nonlinear equations to be solved in the form of *Krasitskii* [1994] and of the methodology. Results from the amplified model will then be discussed in detail. These were obtained by using different initial conditions, different wind speeds, different dissipation terms, and different dissipation "constants." The present work is not intended to provide detailed agreement with experiment, but rather to demonstrate that important qualitative features of wind-driven waves can be obtained. In brief, the principal results are as follows:

1. As noted in earlier work, the nonlinear interactions by themselves produce a marked increase in the high spectral components within approximately one period of the dominant wave. Specifically, components which were initiated at the level of computer noise grow by several orders of magnitude, although they remain several orders of magnitude smaller than the peak of the spectrum. This feature does not change with driving/dissipation.

2. With the growth model to be described below, different wave numbers grow at different rates. After as few as five periods of the initial dominant wave, a new spectral peak develops at a wave number larger than that of that initial wave. The peak shifts toward the red systematically as a function of time. The time dependence of this shift is studied quantitatively in section 3.

3. The spectrum falls off as a power law asymptotically above the wind-driven peak of the spectrum. The exponent of the power law varies only by a small amount as a function of initial conditions and wind speed. It does, however, depend sensitively on the form chosen to model the dissipation. In the course of these investigations it will be seen that if the dissipation is weakly nonlinear, certain initial conditions can lead to numerical instabilities, just as in the case of the models without dissipation. Other initial conditions remain stable, and for these a spectral exponent may be obtained. However, to tame the instabilities, more highly nonlinear dissipation terms are required. The associated spectral exponents depend on the degree of nonlinearity. Ruminations regarding the value of the spectral exponent which emerges from the calculations and its relationship to the dissipation term will be presented in section 5.

4. The Fourier transform (FT) of the velocity potential is computed along with the transform of the wave amplitude. It is found that for wave numbers above the wind-driven spectral peak, this function satisfies a linear theory relation to the FT of the amplitude ($|\psi_k| = C_k\,|\zeta_k|$, a prelude to later notation, where C_k is the phase speed) to a remarkable degree. Thus only the phase speed factor modifies the spectral tail of the velocity potential from that of the amplitude. (When there is little chance of ambiguity, the FT of the potential and amplitude will be denoted as simply the potential and amplitude.) As will be seen, this is because the intrinsic nonlinear dynamics remains truly "weakly nonlinear."

5. The probability distribution function (pdf) of the wave amplitude $h(x, t)$ is approximated very well by a Gaussian after as little as a dominant initial wave period when the initial condition is broadly distributed. When the initial condition models preexisting swell, on the other hand, the pdf may under some circumstances remain markedly non-Gaussian even after 200 such periods.

2. Background

2.1. Autonomous Dynamics

Although full details regarding the convolution method will not be reproduced here, it is useful to give an example, which also serves to introduce notation. The convolution theorem states that the convolution of function f with g, denoted $C(f, g; k)$, can be evaluated by using Fourier transforms, denoted F, as follows

$$C(f, g; k) = \int dk'\, f(k - k')\, g(k') = F^{-1}\,[F(f)\,F(g)].$$

One term in the nonlinear temporal evolution equation (see below) for the Fourier component of the wave elevation is (ζ is that component, ψ the Fourier component of the surface velocity potential)

$$I_a(k) = \int dk_1\, \zeta(k_1) \int dk_2\, |k - k_1 - k_2|\, \psi(k - k_1 - k_2)\, \zeta(k_2).$$

Then, directly from the definition of the convolution we have in two steps

$$\int dk_2\, |k - k_1 - k_2|\, \psi(k - k_1 - k_2)\; \zeta(k_2) = C(|k'|\psi, \zeta; k - k_1)$$

$$I_a(k) = \int dk_1\, C(|k'|\psi, \zeta; k - k_1)\, \zeta(k_1),$$

which is itself a convolution. The fact that such convolutions can be evaluated by using FFT programs is what makes the method computationally powerful.

As is wellknown, the equations governing surface waves may be obtained as a set of Hamilton's equations from the energy functional for the problem. The *Krasitskii* [1994] form of these equations is obtained by making a systematic perturbation expansion, with the relevant expansion variable being the wave slope $k\zeta(k)$. The linear theory corresponds to retention of powers of ζ and ψ no higher than quadratic. The first correction term in the Hamiltonian is third order, and the second correction term is quartic. Thus one speaks of "three-wave and four-wave interactions."

It is also wellknown that the three-wave interaction term has no resonances in the limit of deep water ($kh \gg 1$). Thus it may be eliminated entirely by means of a canonical transformation. This transformation has the effect of modifying the form of the fourth-order interaction term in the Hamiltonian, which does contain resonant interactions in deep water (except in one dimension [*Dyachenko and Zakharov*, 1994], although one can be close to resonance, as discussed by *Willemsen* [1998]. However, it is not necessary to perform this transformation. The computational labor of retaining the three-wave interaction is quite small. Therefore in what follows it shall be left intact. The combination of third- and fourth-order interactions retained here corresponds to what would be called a fourth-order interaction had the canonical transformation been performed.

Coefficients to be displayed below apply in the limit of deep water, and in the absence of capillary effects. Very interesting direct numerical simulations within the framework of Boussinesqu equations have been performed by *Pushkarev and Zakharov* [1996, 2000] retaining capillarity and finite water depth, but these cases will not be discussed here.

To this order, then, the Krasitskii equations in deep water explicitly read

$$\frac{\partial \zeta_k}{\partial t} = |k|\,\psi_k - \frac{1}{2\pi}\int dk_1\,[|k|\,|k_1| - k\bullet k_1]\,\psi(k_1)\,\zeta(k - k_1) - \int\int dk_1 dk_2\, K\zeta(k, k_1, k_2)\,\psi(k - k_1 - k_2)\,\zeta(k_1)\,\zeta(k_2) \qquad (1a)$$

$$\frac{\partial \psi_k}{\partial t} = -g\,\zeta_k + \frac{1}{4\pi}\int dk_1 [k_1 \bullet (k - k_1) + |k_1|\,|k - k_1|]$$
$$\psi(k_1)\,\psi(k - k_1)$$
$$+ \int\int dk_1 dk_2\, K_\psi(k, k_1, k_2)\,\zeta(k - k_1 - k_2)$$
$$\psi(k_1)\,\psi(k_2). \quad (1b)$$

In the above, all (wave number) k variables are twodimensional, although for convenience vector notation (e.g., $k \equiv \mathbf{k}$) has been suppressed. (For this work the vectors are actually one dimensional, but nothing changes in the form of the equations. Again to avoid confusion with other workers' nomenclature, dimension here refers to the dimension of the horizontal coordinates and does not include the vertical.) Additionally, g is gravitational acceleration. Since the velocity potential and the displacement are real quantities, their Fourier transforms must satisfy the conditions $\psi(k) = \psi^*(-k)$, $\zeta(k) = \zeta^*(-k)$, where the asterisk denotes complex conjugation.

The integral kernels K_ζ and K_ψ above are explicitly

$$K_\zeta = \frac{1}{8\pi^2}|k|\,|k - k_1 - k_2|\,\{|k| + |k - k_1 - k_2| - |k - k_1| - |k - k_2|\} \quad (2a)$$

$$K_\psi = \frac{1}{8\pi^2}|k_1|\,|k_2|\,\{|k_1| + |k_2| - |k - k_1| - |k - k_2|\}. \quad (2b)$$

Equations (1) and (2) govern the dynamics of the wave field in the absence of driving and dissipation. They are phase-retaining equations and so intrinsically supply information which is suppressed in the very formulation of the Wave Modeling (WAM) type transport equations. They will now be supplemented with expressions for wave growth and dissipation.

2.2. Deterministic Driving and Dissipation

Recall that Hamilton's equations for ocean waves, in the Krasitskii form or in any equivalent form, are both deterministic and energy conserving. Introduction of driving and dissipation terms as appendages onto Hamilton's equations can destroy both of these properties. (To avoid confusion in terminology, recall the elementary harmonic oscillator. Its equations of motion can be derived from Lagrangian as well as Hamiltonian dynamics. Alone the oscillator conserves energy. A damping term is added to the equations of motion to bring the oscillator to a stop in a finite amount of time. This damping term is added in an ad hoc manner to the equations which follow from an energy-conserving formalism. Energy is no longer conserved.)

Modifications of the basic equations which involve statistically fluctuating quantities (for example a fluctuating wind) give rise to "Langevin" equations. These may serve as the basis for a complete statistical mechanical characterization of the system under consideration. Once external statistically fluctuating drive/dissipation quantities are introduced, the system ceases to be deterministic as well as energy conserving. An interesting example of such a procedure was provided some time ago by *West* [1983].

The present author spent a considerable amount of time attempting to amplify the approach developed by West with the goal of obtaining an approximate statistical mechanical framework within which the Fourier transform of the wave amplitude autocorrelation function, commonly referred to simply as "the spectrum," could be derived rather than postulated. At the very least it was hoped that the program would provide independent support for the "random phase approximation" utilized in transport formulations of wave dynamics of the kind elaborated upon in great detail by *Komen et al.* [1994].

A consequence of these efforts was a working hypothesis for further endeavors: all of the essential features of a wind-driven wave spectrum can be derived, at least in a computational sense, through suitable introduction of driving and dissipation terms which are entirely deterministic. In considering the driving, for example, the inertia of the ocean water is so much greater than that of the atmosphere that short-term wind fluctuations impact high-frequency "riders" on longer gravity waves but on average do not contribute to the overall growth rate, at least to first order of approximation. This was observed to be true with SWADE data during the course of a storm [*Willemsen*, 1997].

The situation regarding dissipation is much cloudier. Nevertheless, following *Phillips* [1985] among others (see below), it seems plausible that dissipation occurs throughout the spectral range, although with weight factors such as wave number k to a power required for the term to be dimensionally correct. Roughly speaking, quantities broadly distributed in wave number space are tightly distributed in real space, and this fits a picture in which waves break in discrete groups (at least until the wind is so strong that a foam description with an ill-defined interface becomes appropriate). At the same time the dependence of dissipation on k usually implies that the dissipation is strongest for large k. This too is plausible if one wishes to attain a "mature" sea with wind driving balanced with dissipation in an average sense across the spectrum, because the shortest waves grow the fastest. A quantitative elaboration of these remarks appears later.

2.3. Forcing Terms

As alluded to above, it is important at the outset to distinguish between two separate scientific approaches to the problem of characterizing wave growth and wave breaking. Consider for definiteness the case of wave growth. One may invoke classic fluid mechanics studies by *Jeffreys* [1924, 1925], *Miles* [1957], *Phillips* [1957], *Benjamin* [1959], and more recently *Belcher and Hunt* [1993] and *Cohen and Belcher* [1999]. These works represent first-principle attempts to identify and parameterize the physical mechanisms responsible for wave growth.

In marked contrast to this work, there is a parallel body of research that tries to construct computationally tractable yet realistic models for driving and dissipation based on observation and/or simulation. Again focusing on driving, one may start with *Plant*'s [1982] model based on direct observation. Scaling arguments which lead to a "fully developed sea" with $k^{-7/2}$ asymptotic spectral falloff have been invoked by *Kitaigorodskii* [1983], *Zakharov and Filonenko* [1966], and *Phillips* [1985], to name but a few, in order to fix the functional form of both the driving and dissipation terms. A relatively recent work by *Belcher and Vassilicos* [1997] models dissipation based upon a combination of scaling and statistical ideas in the spirit of Kitaigodorodskii, Zakharov, and Phillips but comes to a rather different conclusion: that the saturated wave number spectrum in the downwind direction decays as k^{-4} rather than $k^{-7/2}$, as observed by *Banner* [1990] and others. That work may contain a number of assumptions which require further justification from the experimental side, but it illustrates how the earlier scaling arguments might be less constrictive than one would think at first sight. In yet another direction, *Al-Zanaidi and Hui* [1984] developed a model for wave growth based upon numerical studies.

The work described in this paper falls squarely into this second camp. The aim is to draw upon reasonable hypotheses for driving and dissipation models and then to use these models within the FFT computational framework in order to describe the sea surface

in a state of dynamical evolution (wave generation, wave dissipation, and fully nonlinear coupling of the wave amplitude and velocity potential). The key point regarding the treatment of dissipation (beyond viscous losses) in this paper is that one is attempting to model the effects of wave breaking in a simple manner. There is no attempt to address the complicated dynamical processes which occur during wave breaking itself.

Note that the two approaches listed above are not mutually exclusive. For example, Belcher and Hunt derive a u_*^2 law for the energy growth due to the wind (where u_* is the friction velocity). This is precisely Plant's form. The difference is that Belcher and Hunt (and other approaches in the same vein) attempt to compute the numerical value of the overall coefficient multiplying u_*^2. The situation here is analogous to introducing macroscopic (hydrodynamic) viscous dissipation with a physically plausible functional dependence, but with a viscous coefficient which must be determined experimentally, and understood only at a more microscopic physical level. Reaching more deeply into the physical plausibility, it may be said that the "viscous dissipation" is a linear approximation to a more complicated dissipation functional of the velocity potential, with the first expansion coefficient identified as "the viscosity" of the fluid.

In truth, there is likely to be no single value for the unknown coefficient for wave growth, as different values will be appropriate depending on things such as the stability condition between the ocean and the atmosphere [*Pierson*, 1990]. The value of the numerical investigation described here is to establish certain bounds within which growth and dissipation coefficients may reasonably lie in order to produce a realistic ocean surface.

2.3.1. Growth terms. Consider the following four essential issues to be dealt with in formulating a phenomenological model for wave growth in response to a wind. First there is the functional form of the driving itself. Next is the problem of parameterizing the wind velocity. Then, one must ensure that the wind drives waves appropriately depending on their phase speed, as will be discussed in more detail below. Finally, one must adequately parameterize the directional properties of the wind.

The growth of a wave field driven by the wind is often described in terms of the growth of the energy, for example, $dE/dt = \alpha(U)\, E$, in which $\alpha(U)$ is a function of the wind speed U. Considering *Belcher and Hunt* [1993]for concreteness, however, the computed growth function may also be written as $\partial\zeta_k/\partial t \propto u_*^2\zeta_k$, where as was previously noted u_* is the wind friction velocity. Note that their calculation was performed in a frame moving at the phase speed of the spectral component ζ_k. This seems a natural starting point for the present modeling effort.

However, since the friction velocity is not necessarily simply proportional to the nominal wind velocity, this form is awkward, for one would like to shift to a "laboratory" frame of reference via the shift $U \rightarrow (U - c_k)$, where c_k is the phase velocity. This is close to the *Al-Zanaidi and Hui* [1984] form, save that they use $U(\lambda)$ to define an appropriate wind speed. For the purposes of this paper, we will simply introduce a "parameter" U (in meters per second) in a driving function similar to that of Al-Zanaidi and Hui. This formulation will be refined in order to make comparisons with experimental data in future work.

An important set of considerations includes the following: the wind should cause waves with phase velocities smaller than its velocity to grow, waves with larger phase velocities may be diminished, and waves with phase velocities opposite to the wave direction should also diminish. To represent these requirements parsimoniously, introduce the angle ϕ between the wind direction and the wave direction, and let the phase velocity always be a positive quantity, i.e., c_k will refer to the wave speed rather than its velocity. This leads us to consider the *Donelan and Pierson* [1987] model for wind driving:

$$\frac{\partial\zeta_k}{\partial t} \propto (U\cos\phi/c_k - 1)\,|U\cos\phi/c_k - 1|\,\omega_k\zeta_k. \tag{3}$$

It is readily verified that this functional form satisfies the aforementioned constraints by virtue of the factor containing an absolute value. The angular frequency factor ω_k renders the expression dimensionally correct. While in $d = 1$ the $\cos\phi$ term can take only the values ± 1, it has nontrivial variability when $d = 2$. The precise specification of the directional term is a matter of debate within the modeling community. The current placement seems logical on the basis of the frame of reference in which Belcher and Hunt, for example, perform their calculations.

A final point applies to all of the numerical examples discussed below. Since the work is in $d = 1$, it is useful to initiate the wave field as a progressive wave in the direction of the wind. In the work of *Willemsen* [1998,2001] it was useful for the initial wave to propagate symmetrically in the right and left directions. Wrap-around boundary conditions in x space (hereinafter called configuration space) enable the right and left moving waves to collide, producing the opportunity to explore interference between opposing waves. In this work, the (FT of the) velocity potential is adjusted in relation to the (FT of the) wave amplitude in such a manner as to achieve the desired progressive wave.

2.3.2. Dissipation terms. Within the present formalism, ordinary viscous dissipation takes the functional form $\partial\psi_k/\partial t = -\nu k^2\psi_k$, where ν denotes the kinematic viscosity. Our goal is to consider suitable additional terms which model wave breaking as a form of dissipation. The approach taken is in the spirit of *Komen et al.* [1984]: one examines candidate dissipation functionals and asks if the resulting spectra are physically realistic and vice versa. These authors initially started with a *Pierson and Moskowitz* [1964] (PM) spectral form but found that this was consistent with a dissipation function that they considered to be implausible. They then substituted a plausible dissipation function and let the spectrum emerge as a result of the calculation. What we will do below is exhibit a range of dissipation functions and their resulting ($d = 1$) spectra. The work is different from that of Komen et al. because we are not working within the transport formalism. Later research will probe the relationship between models of the kind being introduced here with transport models, but this has not been done as of this writing.

A short calculation indicates that the dimension of ψ, denoted $[\psi]$, is L^{d+2}/T. (This follows from the dimension of a velocity potential in configuration space: the dimension of ψ must take into account the dimensionality of the Fourier transform.) Thus $[\partial\psi(k, t)/\partial t] = L^{d+2}/T^2$, and any model term for dissipation is constrained to have this dimension.

We approach the construction of such a term in two steps. First, certainly the combination $\omega_k\psi$ satisfies the dimensional constraints. Then, if we restrict the possible factors which describe the dissipation to include g (gravitational acceleration), wave number k, and ψ itself, we need to construct a dimensionless function of these three quantities. In $d = 1$ we may consider any $f(k^{5/2}\psi/\sqrt{g}\,)$, while in $d = 2$ we may consider $f(k^{7/2}\psi/\sqrt{g}\,)$.

Before proceeding to utilize these observations, it is interesting to note that in earlier times there was no compelling restriction to introduce solely dimensionless quantities into physical theories. The "fundamental constants" of physics and chemistry include the electric charge e, Planck's constant $\hbar$, the velocity of light c, etc. It is within the context of perturbation theory that the dimensionless combination $e^2/\hbar c$, the "fine structure constant," is recognized as a useful parameter in quantum electrodynamics. The parsimonious mathematical description of friction between bodies called for the introduction of a parameter with dimensions, the same for viscosity as already described, and diffusion as well.

Today, however, one dares introduce a new dimensional quantity to describe physical phenomena only when all other possibilities have been exhausted. We proceed with this caveat.

The temptation arises to try to fix the form of the putative dissipation term by using scaling arguments, specifically in the form of *Phillips* [1985]. For example, from equation (1b) one finds that the nonlinear four-wave interaction term scales with wave number as $k^{-(d+2)}$ under the assumption that ψ and ζ scale according to their intrinsic dimensions. Demanding only that the dissipation term scales in the same manner yields function $f(x) = x^{2(d+2)}$.

However, within the linearized theory, $\psi \propto c_k \zeta$ holds dynamically, and it holds to an excellent approximation for large k even when nonlinear terms, driving, and dissipation are included in the calculation. (This result is obtained from the models to be considered below.) The "dynamical" proportionality above leads to a different scaling theory. Let $f(x) = x^{\chi}$. Then matching the four-wave nonlinear term with the dissipation yields the prediction $\zeta^{(3-\chi)} \propto k^{|(d+2)\chi - 2(d+1)|}$, which is quite different from the preceding. It will turn out that the exponent describing the asymptotic power-law falloff of the wave number spectrum is sensitively dependent on the dissipation term selected, as the above scaling argument suggests, but not sensitively dependent on other parameters of a given model. For example, the choice $\chi = 4$ leads to the prediction that $|\zeta_k|^2$ falls off as k^{-16}.

This choice is singled out for illustration because preliminary results revealed that when $\chi = 2$ for $d = 1$, instability set in for a "wind speed" $U = 5$, which is the very "demon" we wish to avoid. Instability does not set in when $\chi = 4$; so the paper deals almost exclusively with this choice. We will find, however, that k^{-16} is far from what is observed in the calculations, which casts doubt on the scaling argument. We will return to a discussion of this argument in section 5 once various initial conditions have been evolved.

2.4. How Do We Know That We Are Actually Driving and Dissipating the Ocean Surface?

As is well known from common practice, a term in the equation of motion for ζ which is proportional to ζ is considered to be a "driving term" if the coefficient is real and positive, despite the fact that ζ is constantly changing sign as a function of time. Similarly, a term is considered to be "dissipative" if the coefficient is real and negative, as in the case of viscosity. However, when a nonlinear term is introduced to represent dissipation, it is not a priori obvious that the term is unambiguously dissipative. It must be demonstrated.

The consistent way of verifying that non-Hamiltonian modification terms are in fact doing what they are supposed to be doing may be found in the Landau and Lifshitz [1960] textbook on Mechanics. Although their argument was supplied for a Lagrangian system, the method is readily adapted to describe a Hamiltonian system. What follows is an example of how the argument works.

Let the unperturbed Hamiltonian describe the linearized theory

$$H_0 = \frac{1}{2}\int dk\, |k|\, |\psi_k|^2 + \frac{g}{2}\int dk\, |\zeta_k|^2. \tag{4}$$

The aim is to compute dH_0/dt in the presence of driving and dissipation terms. Simply carry the time derivatives inside the integrals and apply the equations of motion, which for linear driving and simple viscous dissipation read

$$\frac{\partial \zeta_k}{\partial t} = |k|\ \psi_k + \alpha\omega_k\, \zeta_k \tag{5a}$$

$$\frac{\partial \psi_k}{\partial t} = -g\, \zeta_k - \nu k^2\, \psi_k. \tag{5b}$$

The linear terms cancel in dH_0/dt, and one has left

$$dH_0/dt = +\alpha g \int dk\, \omega_k\, |\zeta_k|^2 - \nu \int dk\, |k|^3\, |\psi_k|^2. \tag{6}$$

The manifest positivity of the integrands demonstrates that the driving and dissipation terms are indeed adding to and subtracting from the energy, respectively. (Of course, $\alpha \rightarrow \alpha(U, k)$ can be negative in the Donelan-Pierson model; the term then describes direct wind-driven diminution of the wave energy. The term $\alpha(U, k)$ should appear inside the integral for that model.)

Of course, one can solve the simple set of equations (5) exactly. The eigenfrequencies are

$$\Omega = (\alpha\omega - \nu k^2)/2 \pm (i/2)\sqrt{[(2+\alpha)\omega + \nu k^2][(2-\alpha)\omega - \nu k^2]} \tag{7}$$

a result which clearly demonstrates the driving/dissipating nature of the added terms. But the point is that the same principles invoked above apply when using the fully nonlinear Hamiltonian with more complicated dissipation terms, which cannot be solved exactly. The proof is a tedious and uninstructive procedure; so it will not be reported here. As discussed by Landau and Lifshitz, it becomes useful to invoke Euler's theorem on homogeneous functions in order to demonstrate the positivity of the integrands involved in the more complicated cases. The only caveats which emerge are that the argument ψ in the function $f(x)$ discussed earlier must be replaced by $|\psi|$ and that only even powers of x are allowed (otherwise one cannot guarantee that the term is dissipative).

3. Illustrative Model Results

The full nonlinear model of equations(1a) and (1b) has been run in $d = 1$, augmented by the Donelan-Pierson driving term, equation (3), with $\phi = 0$, an overall numerical coefficient $\alpha_0 = 0.0125$, and a dissipation term of the form $\beta\{k^{5/2}|\psi_k|/\sqrt{g}\}^4\, \omega_k\, \psi_k$ with coefficient β to be discussed. The functional form corresponds to function "f" discussed earlier being set to $f(x) = x^4$. Recall that this form was chosen because preliminary investigations showed that x^2 was too weak in the sense that the same instabilities which led to this investigation recurred.

The time integrations were done by using Matlab function "ode45," which is a variable time step Runge-Kutta ((4),(5)) solver. Code optimization was not an issue here beyond successfully implementing the FFT techniques, as was discussed earlier.

Before viewing specific scenarios, it is useful to examine Figure 1. This figure portrays the growth time constant associated with the Donelan driving function. The sharp cusps which are observed occur at k - values which are approximately at the positions of the singularities that exist in the time constant (inverse of the driving coefficient) when $U = c_k$. Values of k above a given cusp correspond to modes that can grow in this wind field. Values of k below the cusp correspond to modes that have negative driving terms, that is, waves that are suppressed because they are traveling faster than the wind. These negative time constants are depicted as positive in order to include them in the semilogarithmic plot. The utility of this plot is illustrated by the following example. Notice that when $U = 15$ ms^{-1}, modes right down to $k \cong 0.075$ have experienced at least one $e$fold growth after 1000 s. The e-folding time at $k = 1$ is slightly less than 2 s.

We now turn to examining a series of configurations characterized by initial conditions and wind speeds. Our attention will focus on the evolution of the wave spectrum as a function of time, but it must be kept in mind that the present methods retain full

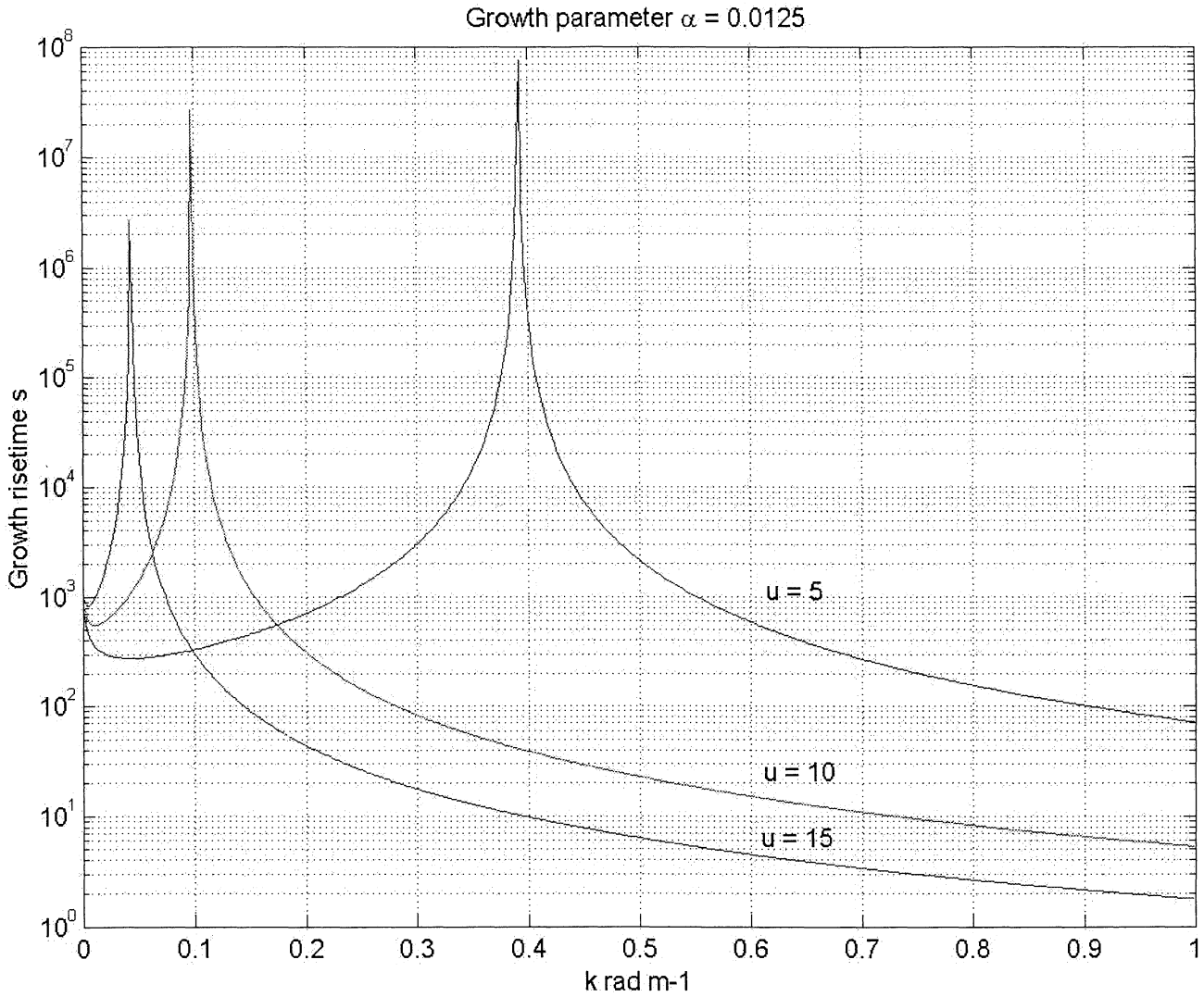

Figure 1. Growth time constant associated with the Donelan-Pierson driving function. Curves labeled U = 5, 10, and 15 m s^{-1} represent one *e*-folding time for wave growth at any given wave number at that wind speed, with the growth parameter $\alpha = 0.0125$.

phase information of the wave field $h(x, t)$, and the velocity potential as well.

In addition, we maintain full information as to the relative strengths of the driving, dissipation, and nonlinear terms. This is useful for evaluating the appropriateness of the truncation of the nonlinear interactions to fourth order. Although detailed results will not be presented, typically after about 1000 s mean wave slopes are of the order of about 0.01, while the maximum slopes are of the order of 0.05. So the system is truly only weakly nonlinear. Direct measures show that the linear terms are of the order of 5 to 10 times larger than the three-wave interaction term, which is in turn of the order of 5 to 10 time larger than the four-wave term. These measures will become even more significant for $d = 2$ because of the existence of true four-wave resonances.

Consistent with the intent of this work, the examples which follow are not always "comparing apples to apples" as when only a single parameter is varied at a time. This type of systematic investigation will be done in the near future. The point here is to illustrate the various "degrees of freedom" which are available for exercising the computational scheme.

3.1. Swell Models

"Swell" models are those that have initial conditions strongly dominated by a single mode of the spectrum. Before proceeding, some detail regarding discretization of the spectrum is in order. The work in this paper has been done with a maximum wave number of 1 m^{-1}, corresponding to a highest frequency of 0.5 Hz. This spectral range corresponds to that encountered in the SWADE data analyzed by *Willemsen* [1997]. The "resolution" is determined by the number of points utilized in discretizing the wave number continuum extending from $k = -1$ to $k = +1$. In this work $n = 1024$ was chosen. This number is close to the limit of memory required to run the calculations efficiently with the present platform.

Because of the discretization, the wave numbers are equally spaced by an amount dk. Now, two different scenarios may arise for swell models: the dominant initial mode can be precisely at one of the discrete wave numbers determined as mentioned, or it can be somewhere in between. (For example, suppose one starts with $h(x, 0) = \cos k_0 x$, where k_0 is not an integer multiple of dk.

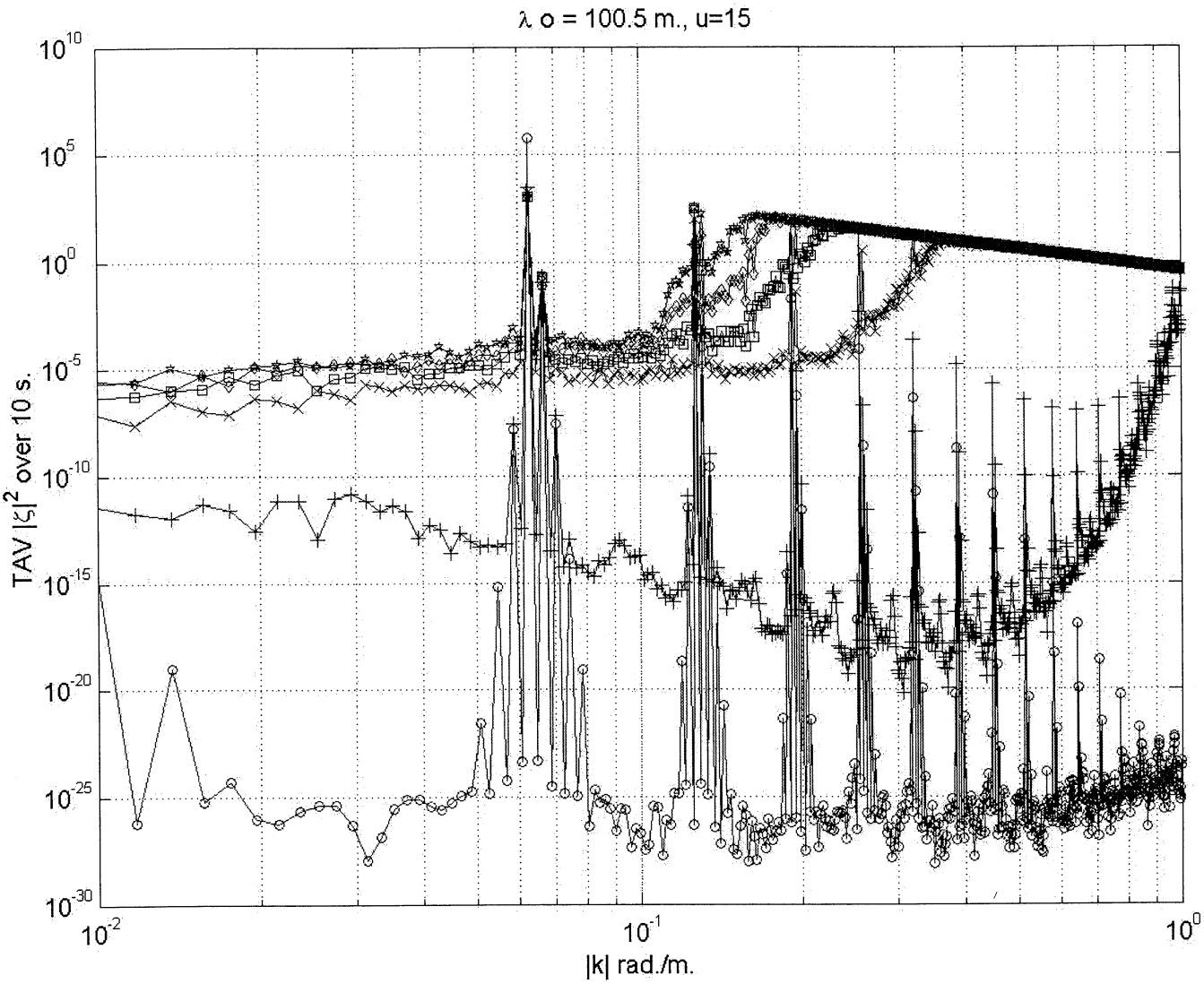

Figure 2. Temporal evolution of the wave amplitude spectrum for an initial swell with $\lambda = 100.5$ m, driven by a wind with speed 15 m s^{-1}. The initial condition is on – lattice. TAV, time averaging. This averaging is performed over a 10 s interval which ends at the times indicated by symbols: 10 (o), 100 (+), 500 (x), 1000 (box), 1500 (diamond), 2000 (star). These times are in seconds.

Its discrete Fourier transform exists but it is not as sharply peaked as when k_0 is an integral multiple.) For convenience a wave number which exactly equals a discretized value will be called "on-lattice."

3.1.1. On Lattice. Let us first consider a model which is on-lattice and in which $U > C_P$, where C_P is the phase velocity at the initial peak of the spectrum. Specifically, we choose U=15ms^{-1} and λ_0 =100.5 m with a corresponding C_P = 12.52 ms^{-1}, and we select the dissipation parameter $\beta = 1$. The condition $U > C_P$ can be re-expressed in the form $k > k^*$, $k^* = g/U^2$. Such modes are driven to grow by the wind forcing term, while those satifying the reverse inequality decay. In the present configuration $k^* = 0.044$ m^{-1}.

Turning to Figure 2, the ordinate is $\langle|\zeta(k, t)|^2\rangle$, where $\langle \ldots \rangle$ denotes the time average over a span of 10s. The figure caption indicates the symbols corresponding to the final time for each curve. The amount of 10 s encompasses multiple periods for almost all of the modes and is thus a suitable averaging time. An average over a greater amount of time runs the risk of being biased owing to nonstationarity of the process under consideration.

The figure displays several qualitative features which all the swell models considered have in common. First, the nonlinear interaction produces strong excitation of harmonics of the initial on-lattice wave number within the first 10 s of the time evolution. Although, as has been mentioned, in $d = 1$ there are no true resonances, it will be convenient in later discussion to discuss such sharp peaks as quasi-resonances (QR). (Also in the future the "time evolution" will often be abbreviated to "the run.") By t = 100s the large k tail has grown by from 7or 8 to approximately 23 orders of magnitude primarily owing to the growth term alone. (From Figure 1, we can estimate the growth as approximately exp (100/2) $\approx$ 5 x 10^{21}.) In addition, the amplitude at the initial spectral peak has diminished by 3 orders of magnitude, but the amplitudes of its harmonics have increased. Nonetheless, some of the QR have been washed out by the surrounding spectral components.

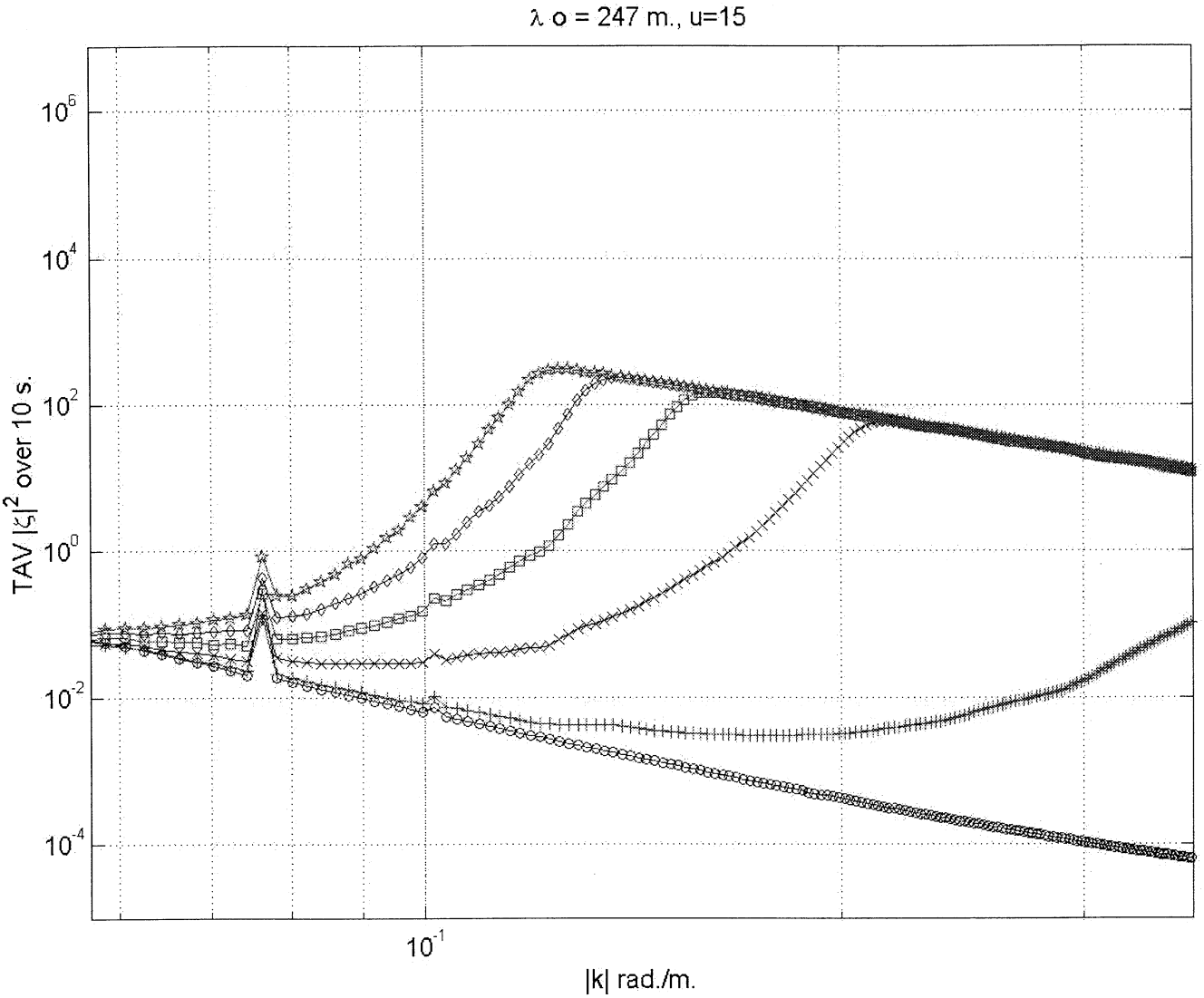

Figure 3. Temporal evolution of the wave amplitude spectrum for an off-lattice initial swell with $\lambda = 247$ m, driven by a wind with speed 15 m s^{-1}. Symbols as in figure 2.

Leaping ahead to 500 s, the entire spectrum has been lifted except at the initial peak, which continues to lose energy. If one considered the driving term alone, one would expect the spectrum below $k^* = 0.044$ to be decreasing, whereas in fact it is seen to be increasing (though remaining very small in comparison with the rest of the spectrum.) This can only be interpreted as an "inverse" cascade from higher wave numbers to lower ones as a consequence of the nonlinear interaction.

Especially striking, however, is that the spectrum "saturates" at wave numbers above appxroximately 0.35, with the largest value at the end of the spectrum coinciding with the highest value achieved at $t = 10$ s. Inasmuch as the growth term is still operational, saturation must be caused by the counteraction of the dissipation term. However, the precise form of the saturated regime must reflect, additionally, the nonlinear exchange among modes. The spectrum below the saturation point is lower. Referring back to Figure 1, the reason at least in part is that the wind has not acted long enough to significantly increase this portion of the spectrum. The net effect is to produce a windinduced peak in the spectrum.

As time increases in multiples of 500 s, the wind peak marches to lower wave numbers. The saturated region maintains its quantitative pattern, with the numerical values coinciding to within the size of the marker symbols. In addition, the resonant values which persisted above the "continuous" part of the spectrum at $t =$ 100 s are swallowed up by the wind and dissipation effects: by the time the wind peak passes to the left of a resonant contribution, its magnitude is no greater than the value of the saturated regime on either side of it.

The saturated regime has been examined separately on a log-log plot. One finds that the data at values of k somewhat above the wind peak are accurately fit by a powerlaw dependence. For example, the $t = 2000$ s exponent was determined to be (-3.32) for $k > 0.37$. Notice that this value implies that the data for $t \geq 500$ s are encompassed by the fit. At the later times, a relatively broad transition regime exists between the location of the wind peak and the onset of quantifiable power law behavior.

Finally, one may inquire into the dependence of the wind induced spectral peak wave numbers as a function of time. From Figure1 one infers that the decrease in k_{peak} as t increases is to be expected. Yet when k_{peak} values inferred from the growth term are superimposed on this figure, it becomes obvious that the quantitative trend is noticeably different from that expected from that term. Treating k_{peak} versus t_{peak} as an independent data set, one

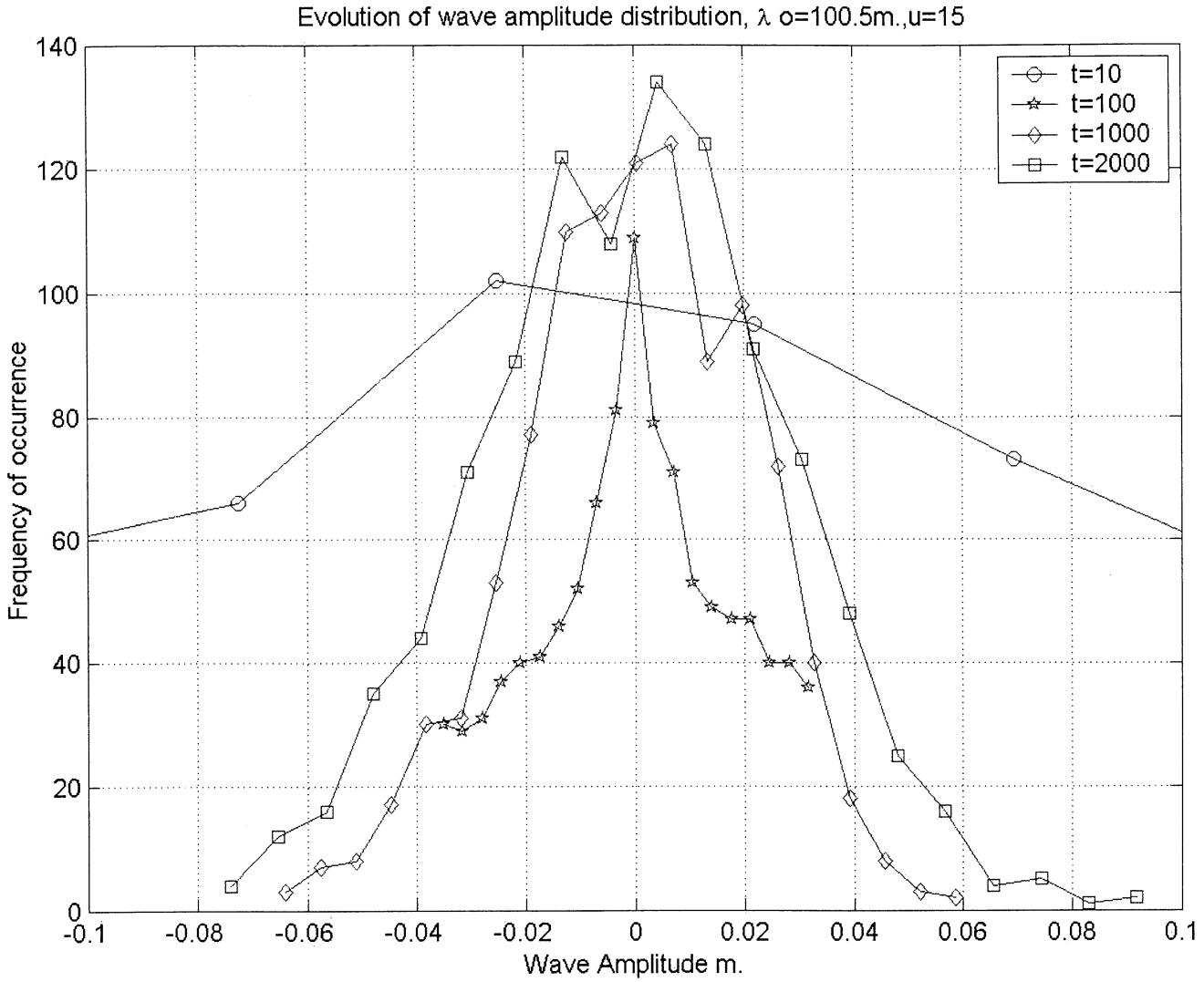

Figure 4. Temporal evolution of a wave amplitude probability distribution function for an on - lattice initial condition driven by a wind with speed 10 m s^{-1}.

finds that the function t_{peak} = (5.61 x 10^3) exp (-6.84 k_{peak}) gives a reasonable fit over the interval t = 500:2000 s.

This functional form is somewhat surprising and must arise from the complete interaction of nonlinear terms, driving, and dissipation (see, e.g., *Hara and Mei* [1991]). It was found that this qualitative behavior is encountered in all of the cases studied, although a graph supporting the goodness of fit will be exhibited for only one case. Thus while the numerical coefficient and the value of the decay constant may be case and model dependent, the qualitative prediction stands a good chance of being tested experimentally.

The results of the preceding paragraphs provide an a posteriori justification for terminating this run, and the others as well, at t = 2000 s. Inverting the functional form, the wind induced peak wave number shifts only logarithmically with time, so it takes longer and longer to shift that peak downward by equal amounts.

The same swell initial condition was run with U = 10 m s^{-1}, so that $C_P > U$. All of the qualitative features observed for U = 15 m s^{-1} occur for this model as well. The principal quantitative differences are that the wind peak is considerably retarded in time in comparison with the U = 15 m s^{-1} case, as is to be expected from figure (1) albeit with the caveats expressed above; the spectrum at wave numbers below the wind peak vary from 7 to 2 orders of magnitude (progression toward smaller k) below the corresponding spectrum for U = 15 m s^{-1}; by t = 2000 s a larger number number of harmonic QR below the wind peak are still present.

A further noteworthy difference is that the 15 m s^{-1} case developed a number of satellite peaks in the vicinities of the harmonic peaks; these are absent for the 10 m s^{-1} case. However, while the satellites are an interesting phenomenon their presence hardly affects the appearance of the sea surface because they are orders of magnitude smaller than the principal peaks. Additionally, since $C_P > U$ the spectrum below $k^*(10)$ = 0.098 $m.^{-1}$ is expected to decrease, for the reasons discussed for the first case. It does not, and this again is interpreted to be a consequence of nonlinear interactions.

The most interesting result from this run is that saturation in the high end of the spectrum (above the wind peak) behaves quantitatively almost identically as it did in the first run. The large-k tail, from k = 0.48 to k = 1, is of power law form with exponent (–3.20) based on the t = 2000 s data. The earlier time data lines up with this later data to within the same accuracy as was shown in Figure 2 for U = 15 m s^{-1}. It seems, therefore, that the spectral exponent is insensitive to the wind speed.

Earlier, reasons were given for selecting the specific dissipation function used in this work: a dissipation function propor-

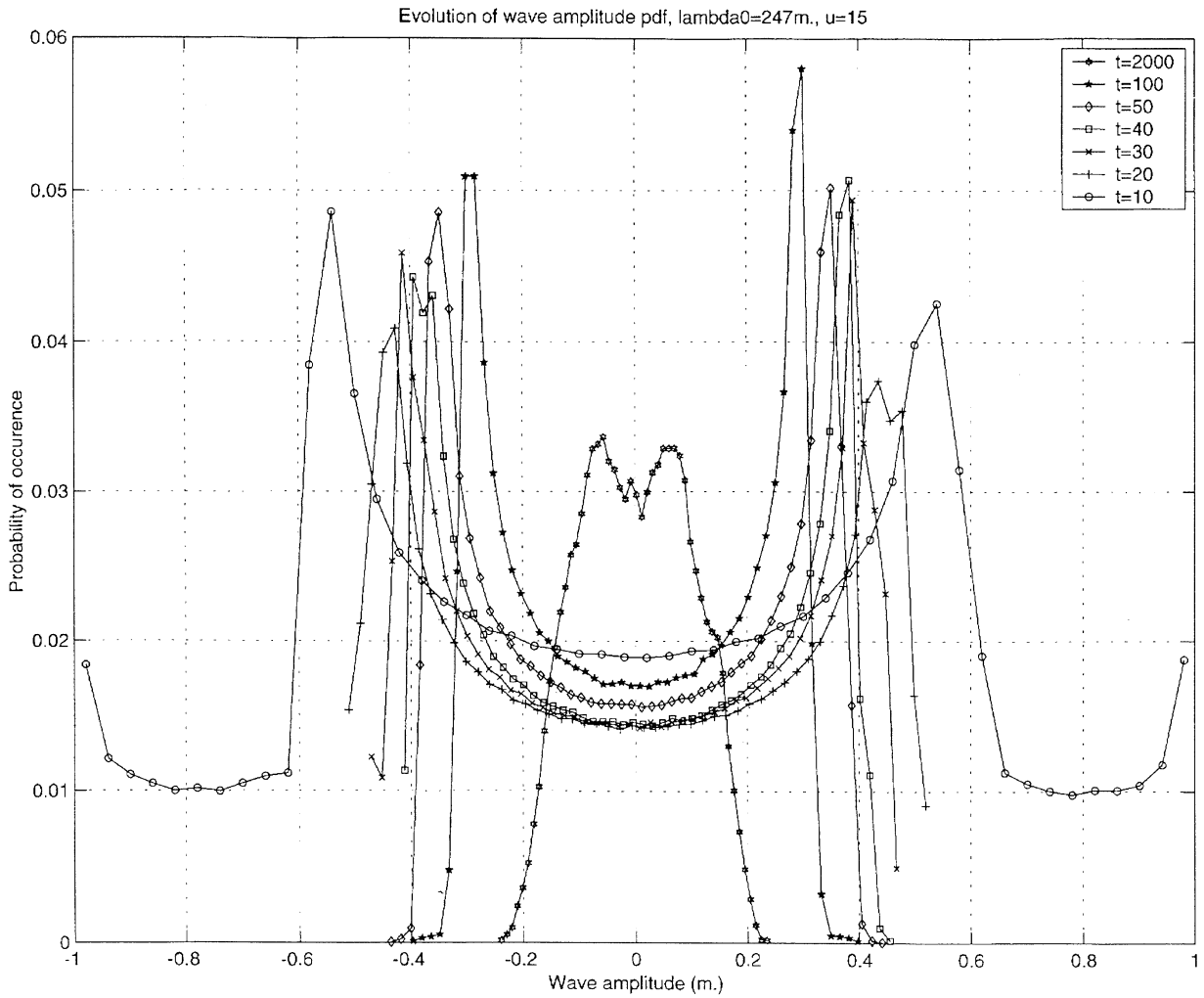

Figure 5. Temporal evolution of a wave amplitude probability distribution function for an off - lattice initial condition driven by a wind with speed 15 m s^{-1}.

tional to $|\psi|^2$ (rather than the $|\psi|^4$ form we are working with) sometimes led to catastrophic high wave number divergences in the calculations. However, it did not always behave in this manner. In numerically stable runs at wind speeds of 10 m s^{-1} and 15 m s^{-1}, for example, spectral exponents with values between (-2.15) and (-2.5) were generated. Thus the spectral exponent does depend sensitively on the precise form of the dissipation function.

The on-lattice swell model has been exercised under several other initial conditions, and all of the results are qualitatively as described for the two above. Most importantly the exponent of the spectral tail remains in the range (-3.2) to (-3.32) and thus appears to be universal within numerical/statistical uncertainties. For example, a significantly different on-lattice swell model with λ_0 = 402.1 m, U = 20 m s^{-1} yields a spectral exponent of (–3.32), the same as for the first case within roundoff, for a range beginning at k = 0.13 m^{-1}.

3.1.2. Off Lattice. Next, consider swell which is off-lattice, that is, the dominant wave number does not correspond to one of the discretized values of the model. Again one may envision a wide variety of initial conditions, but here only a single case will be reported in order to demonstrate the differences which arise vis a vis the on-lattice models.

The case to be considered is U = 15 m s^{-1} and λ_0 = 247 m (admittedly a very long wavelength, but one wishes to explore limiting cases). This wavelength corresponds to k = 0.0254, which is close but not exactly equal to a lattice wave number with the discretization described at the beginning of this section. A consequence is that the discrete Fourier transform of, say, cos k_0x, is peaked about lattice values close to k_0, but it has much broader shoulders than if k_0 was an on-lattice value.

Figure 3 displays the spectral evolution of this model. Comparing with figure 2 both similarities and differences are evident. In no particular order of importance, the qualitative similarities are as follows: progression of the wave peak toward the red as a function of time, the formation of a saturation regime onto which all of the curves coincide, and quasi-resonance formation as a consequence of the nonlinear interaction. Qualitative differences include a striking reduction in the number of QR which are excited: note that none are excited at all below the swell peak. A curious data collapse occurs between the initial swell peak and its first quasi-resonant excitation which was not present in on-lattice models, and overall there is a much smoother structure.

Quantitatively, the spectral exponent for this model is (–3.33) for k > 0.37. This exponent is consistent with the on-lattice models, reinforcing the suggestion that it is universal. The temporal evolution of the wind peak wave number is again found to be of exponential form, but the parameters are different: t_{peak} = (1.22 x 10^4) exp (-15.11k_{peak}). Comparing Figure 3 with Figure 2, it is evident that the wind peak is approaching the swell spectral peak at a much slower rate in the off-lattice case than in the on-lattice

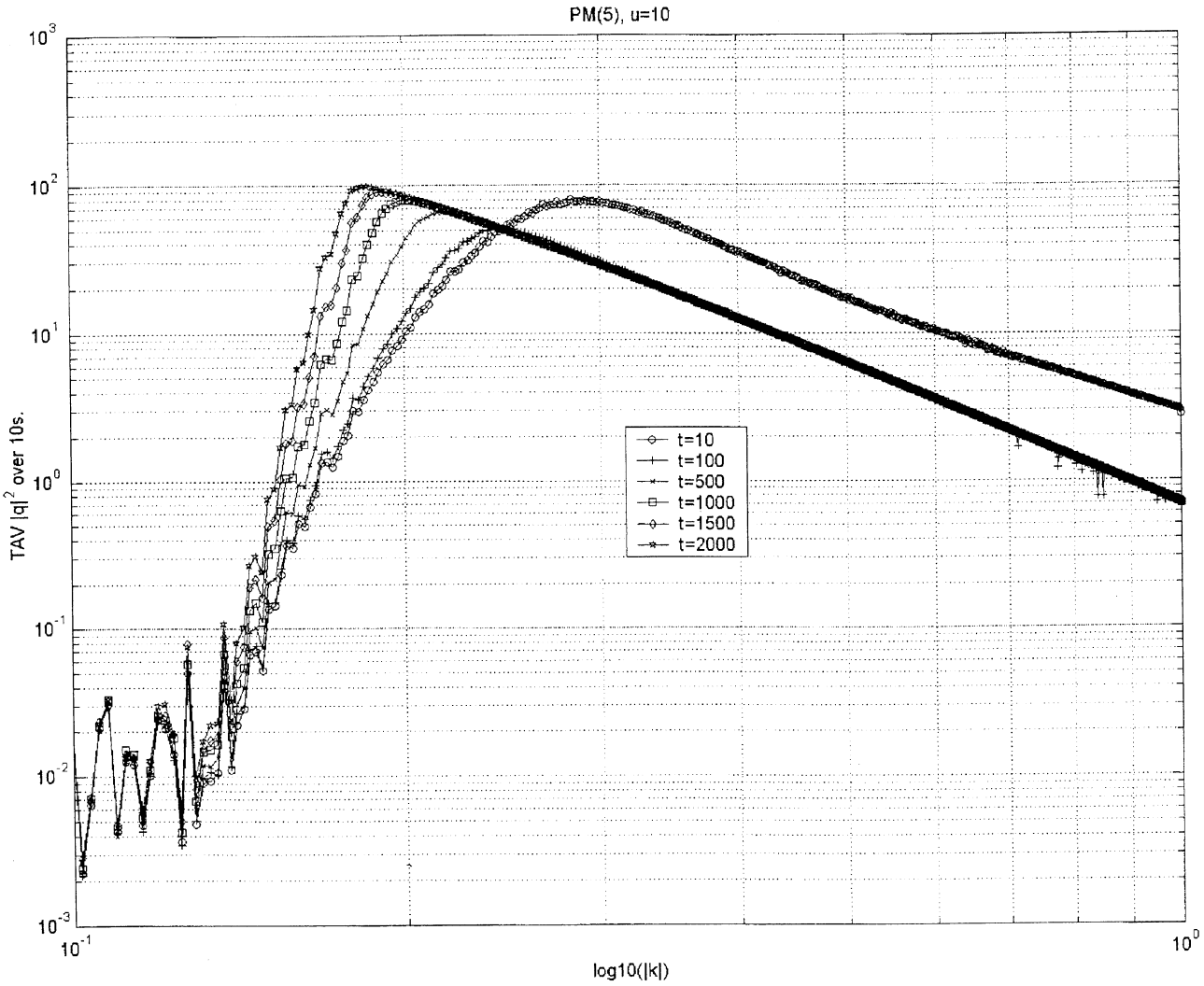

Figure 6. Temporal evolution of the wave amplitude spectrum for an initial "Pierson-Moskowitz" spectrum calculated with parameter $u = 5$ m s^{-1}, driven by a wind with speed 10 m s^{-1}.

case, even though the wind speed $U = 15$ m s^{-1} in both cases. This, together with earlier observations regarding the QR, suggests that the resonant effects of the nonlinear interaction are suppressed in the off-lattice case. It further suggests that resonant effects play a significant role in the approach to full development at a given wind speed.

To conclude the discussion of swell models, we look at examples of the evolution of the probability distribution function of the wave amplitudes. Figure 4 applies to the on-lattice model $U = 10$ m s^{-1} and $\lambda_0 = 100.5$ m. The times in this figure are nominally 10 s, 50 s, 100 s, and 2000 s in order of decreasing magnitudes at the $h = 0.05$ gridmark. The times are "nominal" because all of the amplitudes in the 10 s interval below the nominal value are included in order to improve statistics. The behavior consists of a contraction of the wave amplitudes over time, starting from a very broad and multimodal distribution (the t = 10 s case is much broader than the figure indicates, extending to approximately ± 0.5 m) and evolving into a narrow, smooth distribution suggestive of a Gaussian. An attempted fit reveals, however, that the shape is not truly Gaussian, although it is close.

Figure 5 refers to the off-lattice model and reveals two interesting properties of the corresponding distribution. It also starts as an essentially bimodal distribution (positive and negative amplitudes corresponding to the initial condition). However, it maintains this bimodal structure, changing significantly over the first 100 s of the run as the wave height range diminishes. The second point of interest is that subsequent change in the shape of the pdf occurs comparatively slowly between 100 s and 2000 s. Even at that late time the pdf has not entirely lost its bimodality.

These two very different observations beg for quantitative comparisons with experimental data. This will be attempted in further work. To anticipate later comments, in nature it is much more likely that one will encounter off-lattice swell than on-lattice swell; that is the initial swell will rarely be peaked about a single wave number. Thus the second numerical experiment may behave qualitatively more like what one is likely to encounter in a field experiment than the first one. If the second scenario is accurate, the implications for predicting extreme events are far from trivial.

3.2. Broad Initial Spectra

The initial spectra used in this subsection are loosely based on a *Pierson and Moskowitz* [1964] form. They will be labeled as PM, although it would be a stretch to claim that they are PM spectra one would use to describe experimental data. The functional form used is the same as in the work of *Willemsen* [2001]:

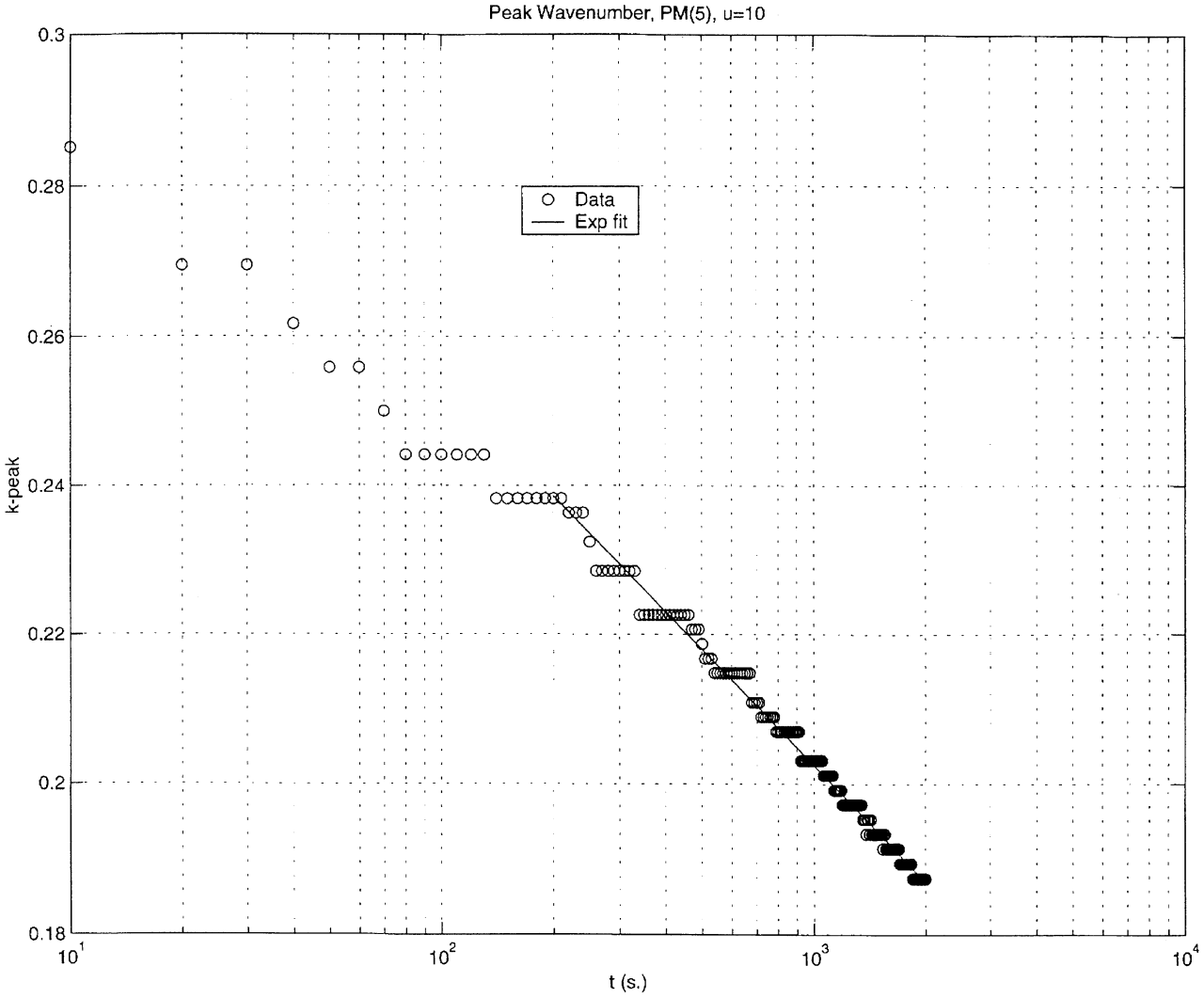

Figure 7. Shift of the wind peak in the spectrum as a function of time for a PM (5) initial condition driven by a wind with speed 10 m s^{-1}. The solid line represents a fit to the data described in the text. Notice that the fit is good over an order of magnitude in time.

$$F(k) = W_0 k^{-\beta} \exp(-\alpha/k^2).$$

The parameter α equals a constant α_0 divided by wind speed U^4. (It is not to be confused with the wind driving parameter of the same name.) For all of the cases described below, the value of U used in this formula is 5 m s^{-1}. This leads to the selection α_0 = 168 so that the spectral peak occurs at the value of k such that the phase speed equals U. The exponent β used in this formula is chosen to be 7/2. (Again, it is not to be confused with the dissipation coefficient.) Overall this choice of parameters gives rise to a curve which is smoothly varying with a weak maximum and a very small domain in which power law fall off is dominant.

The initial wave amplitude spectrum is defined by using $\zeta_k \propto \sqrt{|k|^{1/2} F(k)}$, with the extra power of k arising from the relation between ζ and the wave action. Inasmuch as "pure" PM initial conditions as defined here lead to very cuspy wave shapes in configuration space, the ζ_k are assigned random phases. This produces a very choppy initial wave field. Consequently, the overall constant of proportionality is chosen so that the maximum slope of the initial wave field is not too large. For the cases discussed below, the maximum initial slope was set to 0.1.

There is a further change in this set of models which involves the dissipation parameter β. Inasmuch as the value β = 1 used for the swell models led to very rapid damping of the wave fields at the onset of the runs, a value β = 0.125 was introduced into this set of runs in order to evaluate the differences this produces. Further discussion of the consequences of varying β is reserved to the next section. For now, suffice it to say that rapid damping still occurs and that the important qualitative features encountered in the swell models occur here as well.

Reverting to the use of U as defining the imposed wind speed, the first case considered is defined by U = 10 m s^{-1}. Examination of figure 6 indicates that red shifting of the wind peak as a function of time, saturation of the spectral tail, and the prospect of asymptotic power law falloff are all present in this model. Differences from the swell models include a descent (rather than an ascent) from the initial spectrum into the saturated spectrum, stimulation of QR only in the region below the wind peak, and an apparently much more narrow spectral range. This latter is in fact merely a consequence of the absence of an overriding swell peak. Inspection of the swell cases in retrospect reveals that the wind-sea spectral range is of the same order of magnitude as that in this figure.

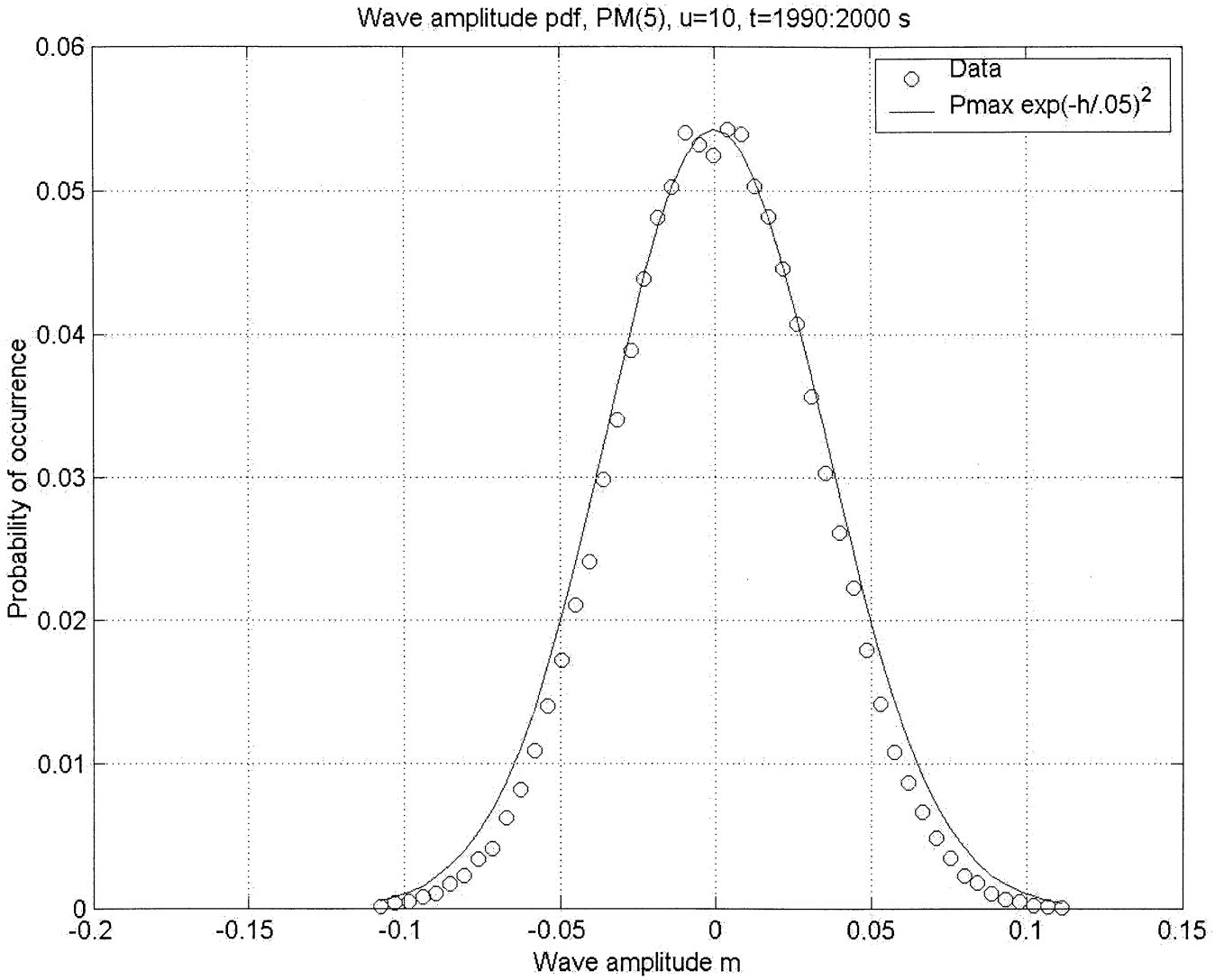

Figure 8. A typical wave amplitude pdf within the class of PM initial conditions. Particulars are indicated in the figure.

Quantitatively the power law falloff as calculated from t = 2000 s data starts from k = 0.58, thus encompassing the earlier time spectra. The spectral exponent is (–3.22). Evidently the value of the spectral exponent does not depend on whether the initial condition is swell or broadly distributed.

In addition, the temporal advance of the wind peak toward the red is again exponential: $t_{peak} = (8.39 \times 10^6) \exp(-44.6 k_{peak})$. The range and validity of this fit may be evaluated from Figure 7. An inevitable distraction is that for closely spaced times the precise positions of the wind peaks in k-space may lie so close together that they cannot be resolved. This phenomenon is what gives rise to a sequence of plateaus in the data: they are an artifact devoid of physical significance.

The pdf for this case is persistently Gaussian from early times. Figure 8 shows an approximate fit which gives an idea as to the validity of such a functional representation. Hower, random phases were assigned to the spectral components in the first place, so it is plausible that this resulting form for the pdf is "built in."

The PM (5) initial condition was subsequently exercised at U = 15 m s^{-1}. The spectral exponent in this case was found to be slightly different from the preceding, taking a value of (–3.34) starting from k = 0.51. Surprisingly, however, to within roundoff errors the expression for the temporal advance of the wind peak is identical to the case U = 10 m s^{-1}. A difference is that the range of the fit extends all the way from t = 10 s to 2000 s, extrapolating accurately beyond the range in which it was initially computed. In addition the "goodness of fit" is quantitatively better, with fewer and less pronounced plateaus.

Figure 9 completes this section. It is an example of yet another method of visualizing data that could be applied to any of the other models as well. To explain the figure, recall that the calculational method produces functions $\zeta(k, t)$. For each k and for the range of t indicated in the figure, one may calculate the FT with respect to t, yielding a new function $\zeta(k, \omega)$. The modulus squared of this function is a surface represented by contours in the figure after the replacement $f = \omega/2\pi$. The outermost contour represents a threshold value so that smaller values are suppressed from the graph, hence the narrow range in k.

The first significant feature of this figure is the very clear asymmetry which exists between positive and negative f. The interpretation of this asymmetry is rooted in the observation that within the linear theory, the argument of the wave field (kx - ωt) represents a right moving wave, in the direction of the wind. The existence of (a much smaller number of) left moving (negative frequency) waves does not seem physically unreasonable, but it will require more work to thoroughly understand how they arise within the calculations.

Visualization of a second significant feature has been enhanced by the insertion of two continuous curves at positive and negative frequencies. These curves represent the linear dispersion relation

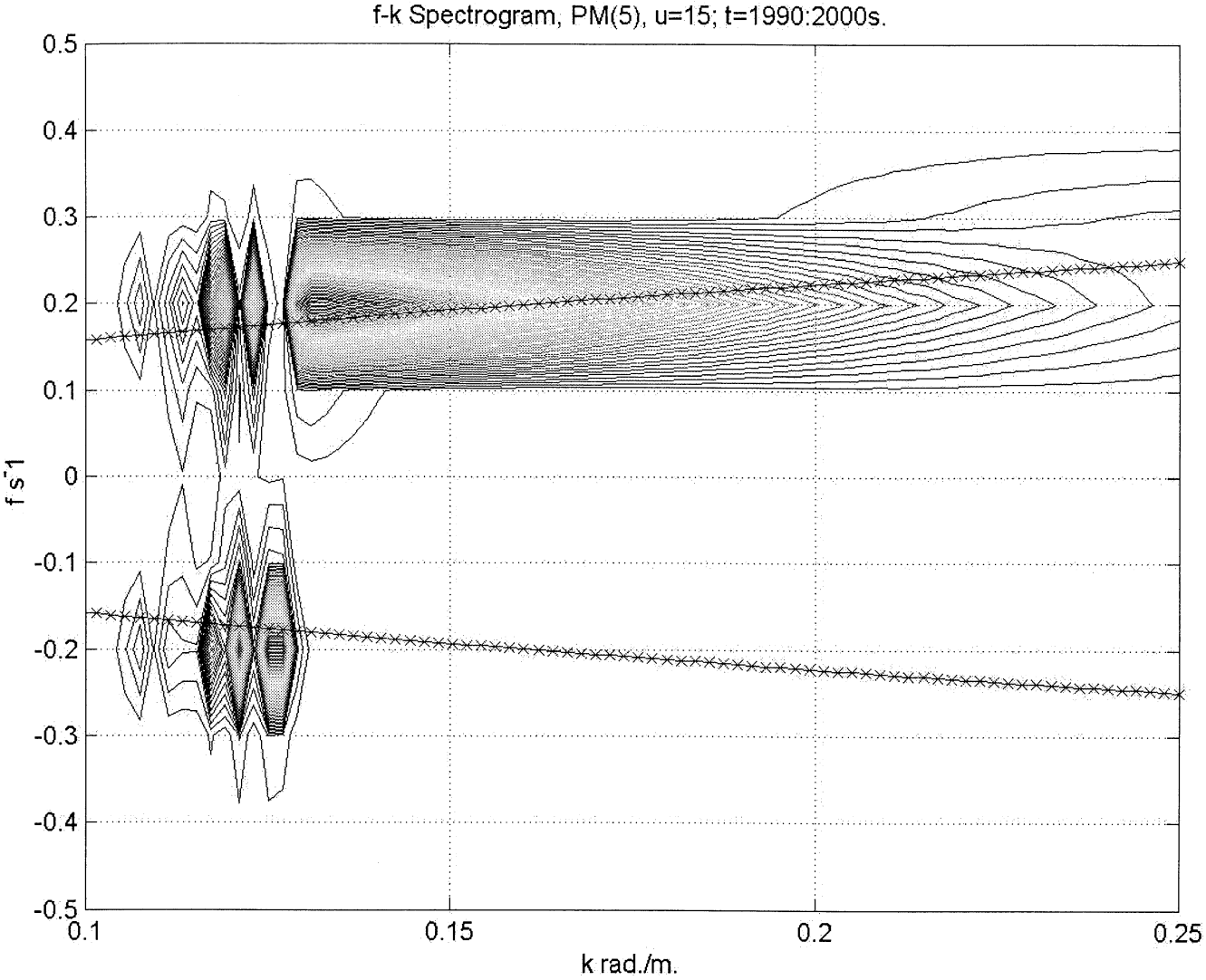

Figure 9. Wave number-frequency contours for a PM (5) model driven at 15 m s^{-1}. The crosshatched lines indicate the linear dispersion relation $2\pi f = \sqrt{g|k|}$.

$2\pi f = \sqrt{g\,|k|}$. In the work of *Willemsen* [2001] the frequency spectrum at each k was also computed, but it was found instructive to display the results in a different manner. The peak frequency at each wave number was determined and from this an effective phase velocity was computed. These were plotted as a function of k to exhibit deviations from the linear theory. The deviations can be understood in terms of mode mixing. The complexity displayed in figure 9 suggests that such a simple comparison is not likely to prove fruitful in the presence of driving and dissipation. For one thing, the maxima of the contoured function are significantly shifted away from the linear dispersion relation, both for right and left moving waves. Even more striking is a visually obvious alignment of the positive frequency contours along an axis which is flat as a function of f. No clear theoretical explanation for this alignment has yet come to mind.

4. Further Exploratory Calculations

The results discussed above have centered about a few well-posed features of the time developing wave spectrum. However, as discussed in *Willemsen* [2001], one has the ability to monitor the magnitudes of the third and fourth order nonlinearities as functions of wave number and time (examples were discussed earlier), to study the instantaneous driving and dissipation functions, and to study the overall energy and action evolution of the system. That is, each separate contribution to the time derivatives of ζ and ψ can be examined in isolation to assess its relative role, as well as the ensemble behavior which manifests in global quantities. Of course one may also examine the wave field and the velocity potential in real space and time. It would be erroneous to believe that the full richness of data which the computational method supplies has been explored within this paper.

In addition the work in this paper has been restricted to a non-fluctuating wind field for reasons cited earlier. Along with this, a steady wind throughout the course of the calculation has been assumed. Incorporation of new features (wind drift at first, wind fluctuations if deemed necessary) is completely straightforward, and it will be done in future investigations.

Having stated these caveats regarding the scope of the present work, it remains for us to tie up a couple of loose ends germane to the actual work that has been described.

First, it is interesting to ask what happens if the wind is suddenly turned off after acting for the length of the runs reported. Figure 10 displays the results when a $U = 15$ m s^{-1} wind acting on the PM(5) initial spectrum is removed after
2000 s. The figure contains 50 separate curves, each one corre-

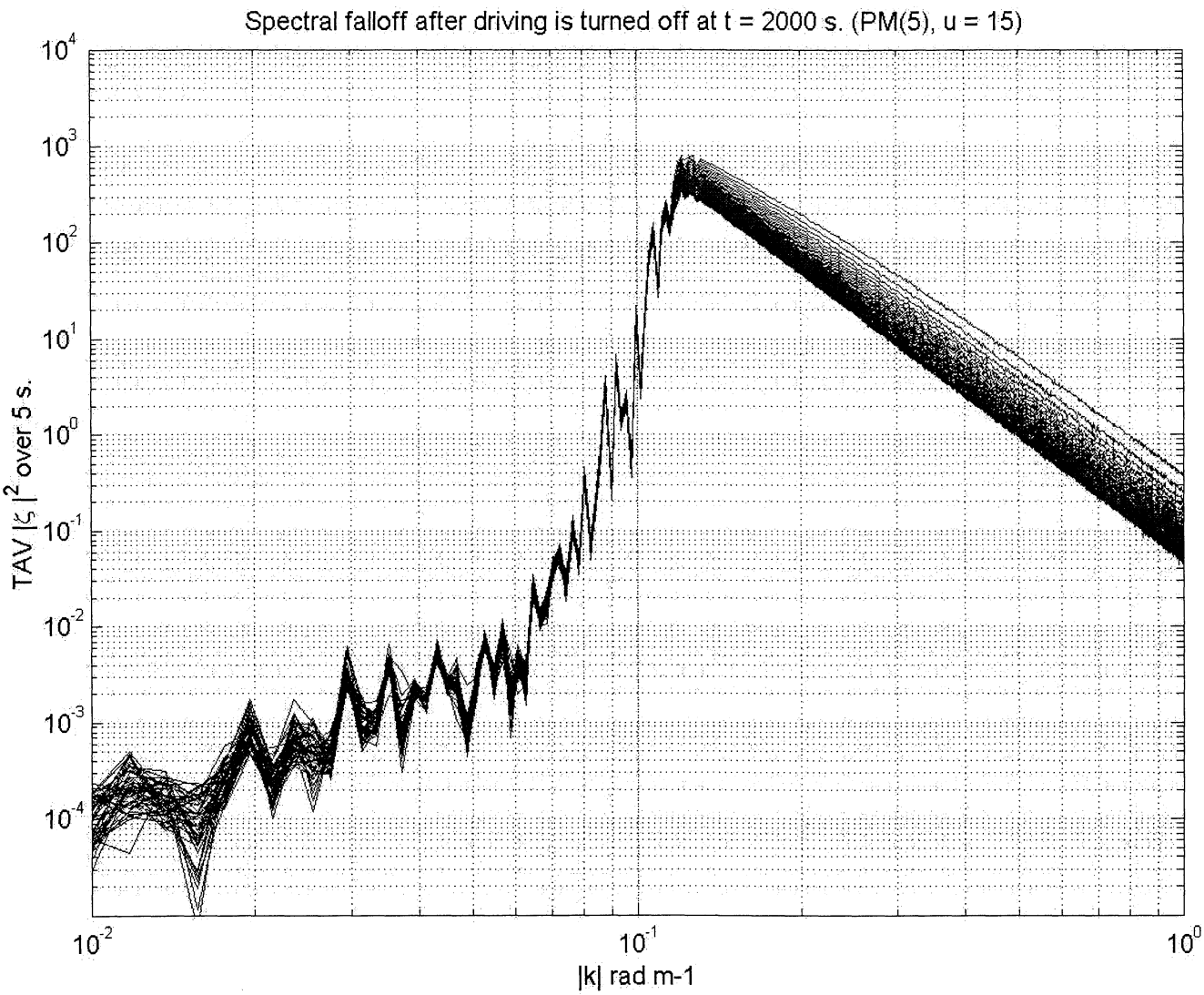

Figure 10. Compilation of data demonstrating the falloff in the spectrum of a PM (5), u = 15 m s^{-1} run when the driving term is shut off ($\alpha = 0$) after 2000 s of evolution from the initial condition. The lines represent time averaged spectra at times 10, 20,...., 500 s after shutoff.

sponding to a time average over 10 s at 10-, 20-, ..., 500 s endpoints after removal of the wind. The curves have been superimposed in order to emphasize the remarkable lack of change over approximately a factor of 2 in k-space just under the spectral peak; and also to show that the spectrum above the peak appears to "pivot" about the peak value. Quantitatively one finds that the tip of the cascade behaves as $\langle|\zeta(t, k_{max})|^2\rangle = 0.34\ t^{-0.54}$ for t in the interval 20-500 s after shutting the wind off.

This falloff implies that the spectral exponent also changes with time. At the latest time considered, t = 500 s, this exponent had declined to a value of (-4.28). Similar results are obtained for different initial configurations. For example PM (5) with U = 10 m s^{-1} shows a $t^{-0.53}$ falloff for the tip of the spectrum, and a spectral exponent of (-4.29) after 500 s.

Finally, the case PM (5), U = 10 m s^{-1}, was recomputed by using parameter $\beta = 0.0625$, that is, half the value discussed earlier. There were no qualitative changes in any of the spectral properties that have been examined. As is to be expected, the spectral levels are higher with the smaller damping parameter. In the region of the spectral tail the quantity $|\zeta|^2$ is larger by approximately a factor of 2. The slope of the tail did not change. This is most convincingly visualized by plotting the ratio of the results (not shown): this ratio is flat as could be over the range of the power law fit.

5. Summary, Conclusions, and Future Directions

The results which have been discussed represent a solid advance toward achieving the goal of being able to calculate a wind-driven sea spectrum ab initio. Such a spectrum should exhibit a spectral peak determined by the acting wind, a power law tail which is in agreement with experiment, and directional characteristics which must also be in agreement with experiment. The first two features have been attained qualitatively; more work involving tuning of parameters will be required in order to make comparisons with field data.

The Donelan-Pierson driving function successfully produces a wind peak in the spectrum which migrates to the red as the wind forcing persists. The precise numerical coefficient can and should be adjustable to accommodate differences in air/sea properties which go beyond wind speed. For example, *Donelan* [1999] utilizes different overall numerical coefficients for favorable and unfavorable wind-wave configurations. Yet another issue to be

addressed in future work concerns the appropriate choice of the nominal wind speed U to be used in the calculation in terms of a measured wind speed.

An important aspect of the driving function which was not treated in this paper is that the directional properties of the spectrum will follow directly from the formulation. There is no freedom to massage the spectrum which emerges once the model is exercised in $d = 2$. No problems of principle block implementation of calculations in that dimensionality. The stumbling block at present is computational resources: $n = 1024$ in $d = 1$ amounts to a 32 x 32 lattice in $d = 2$, which is too small to give reliable information.

The dissipation function utilized in this work was constructed in the time-honored manner of invoking dimensional analysis on the variables considered to be germane to the dissipation process. In more detail, however, a specific form of the function $f(k^{5/2}\psi/\sqrt{g}\,)$ was adopted, namely, the fourth power of its argument. The available numerical evidence suggests that this choice is the overriding determinant of the asymptotic spectral exponent.

Further interesting quantitative results emerged from analyzing the results of the numerical computations. One is the logarithmic law governing the shift of the wind peak as a function of time in the presence of a steady prolonged wind. While the parameters of the fit were found to be very dependent upon the case under consideration, the qualitative dependence held in every case. It is hoped that this prediction can be checked experimentally. In future work the shift of the peak under variable conditions will also be analyzed.

One issue regarding wave aging which the present work does not address is the shift of the overall amplitude of the spectral tail by a factor U/c_P (wind speed over peak phase speed) raised to a power as discussed, for example, in *Banner* [1990]. A possible reason for not detecting this trend in the present calculations is that the wave number range is about an order of magnitude lower than the data examined by Banner.

A second interesting observation regards the "pivoting" of the spectral tail about the initial wind peak once the wind forcing is removed. The power law decay of the high wave number tip of the spectrum as a function of time implies that the magnitude of the spectral exponent increases with time. Again, it would be very useful to analyze data with this prediction in mind. Recall also that the region of the spectral peak did not respond very rapidly to the elimination of the wind forcing. This is qualitatively in accord with the well-known persistence of swell for very long times.

Additionally, the scaling of the FT of the velocity potential with the FT of the wave amplitude for wave numbers above the wind peak presents both experimental and theoretical challenges. Has this scaling been observed? Why is a simple relation from linear theory so accurate in the presence of nonlinearity, driving, and dissipation? This is especially intriguing in light of Figure 9, which shows strong deviations from the linear dispersion relation.

We have also seen that a considerable range of values of the dissipation parameter β is permissible without changing any important features of the spectrum and its evolution. This said, however, the results reported above do suffer from what could be a serious quantitative problem. It is that the dissipation term reduces the energy in the system dramatically over the first 10 s or so in every run that has been conducted. This is not in good qualitative agreement with experiment.

A degree of "ramping up" of the dissipation term exists within the present formulation in the following sense: the "new" dissipation term is of comparable magnitude to the viscous dissipation term when $|\psi|$ is of order $\nu k^{-17/8}$. In the saturated regime we have found $|\psi_k| = c_k\,|\zeta_k|$ with $|\zeta_k| \propto k^{-3.25/2}$ (taking the spectral exponent in the middle of its observed range for the sake of argument). Thus focusing solely on the wave number dependence, at times before saturation is reached the viscous dissipation term dominates, while after saturation the two terms are comparable.

However, the viscosity ν is very small numerically (10^{-6} m^2 s^{-1}), so the new dissipation term soon overwhelms viscous losses. This would suggest that a dramatically smaller dissipation coefficient β might be required for the system to gain energy from the wind significantly before losing it to dissipation. Utilization of a very small value of β might, however, cause instabilities to reappear. Balancing growth rates and dissipation rates in a more realistic fashion is the most important goal for future research.

Finally, to focus this goal, note that "observation" of a spectral exponent as a consequence of temporal evolution within the current computational scheme is interesting: but why does the exponent take the value that it does? In section 2 the possibility of invoking Phillips-like arguments which tie together the scaling properties of the nonlinear, driving, and dissipation terms was mentioned. Recall, however, that one arrives at very different results depending on whether ψ scales like its intrinsic dimension, or like its "dynamical dimension," found to be $c_k\zeta$.

To demonstrate the Phillips-like approach in detail, assume we are in the asymptotic scaling region so that if $k \rightarrow \lambda k$, with λ a scale factor, $\zeta \rightarrow \lambda^{-\rho}\zeta$. The dynamic scaling property of ψ leads to $\psi \rightarrow \lambda^{-\rho-1/2}\psi$. Then in abbreviated form, the scaling behavior of equations (1a) and (1b) supplemented with the driving and dissipation terms for transverse dimension d is

$$\frac{\partial \zeta_k}{\partial t} \rightarrow \lambda^{-\rho}\,[\ \lambda^{1/2} + \lambda^{d+3/2-\rho} + \lambda^{2d+5/2-2\rho} + \alpha(\lambda k, U)\,\lambda^{1/2}\ ] \qquad (8a)$$

$$\frac{\partial \psi_k}{\partial t} \rightarrow \lambda^{-\rho}\,(\ 1 + \lambda^{d+1-\rho} + \lambda^{2d+2-2\rho} + \nu\,\lambda^{3/2} + \beta\,\lambda^{4(d+1-\rho)}). \qquad (8b)$$

A word of explanation is in order. The first term of the right hand side of equation (1a) is $|k|\psi_k$. If $k \rightarrow \lambda k$, the term becomes $\lambda(\lambda^{-\rho-1/2})\,|k|\psi_k$, whence the term $\lambda^{-\rho+1/2}$ in equation (8a). The nonlinear terms' scale factors include those of the fields, the integrals, and the kernels.

Consider first the exponents of the three-wave and four-wave nonlinear interactions in equation (8a) in $d = 1$. They are equal if $\rho = 2$, which coincides with the so-called "old Phillips spectrum" albeit for the wrong "d." In this case the entire nonlinear source term for $\frac{\partial \zeta_k}{\partial t}$ scales as $\lambda^{-3/2}$ except for the implicit dependence within the function $\alpha(k, U)$. (For very large k this scales as $1/c_k^{\,2} \rightarrow \lambda/c_k^{\,2}$ but within the range of k studied in this paper that asymptotic scaling is not realized.) In addition, with this value for ρ the entire nonlinear source term for $\frac{\partial \psi_k}{\partial t}$ scales as λ^{-2} with the exception of the viscous dissipation term, which we have already argued is numerically insignificant. It would appear, then, that consistent scaling of all of the principal terms in the equations of motion has been achieved. Unfortunately, however, in $d = 1$ we have found that the scaling exponent $\rho \approx (3.2 \text{ to } 3.3)/2$.

The way to proceed under this circumstance is to insert the observed value into eqations (8a) and (8b). The result is surprising and intriguing if not necessarily comforting. If for definiteness the value ρ precisely equal to 1.6 is inserted, one finds

$$\frac{\partial \zeta_k}{\partial t} \rightarrow \lambda^{-1.6}\,[\ \lambda^{1/2} + \lambda^{0.9} + \lambda^{1.3} + \alpha(\lambda k, U)\,\lambda^{1/2}\ ] \qquad (9a)$$

$$\frac{\partial \psi_k}{\partial t} \rightarrow \lambda^{-1.6}\,[\,1+\lambda^{0.4}+\lambda^{0.8}+\nu\,\lambda^{3/2}+\beta\,\lambda^{1.6}\,]. \qquad (9b)$$

The result is that there is no matching of scaling exponents among all of the relevant terms. Rather, there is a single term which dominates all others in either equation, and it is the β-dependent dissipation term. Referring to equation (8b), this corresponds to the choice $5\rho = 8$ when $d = 1$. If the slightly larger value $\rho = 1.65$ is inserted instead, the result is qualitatively the same, except that the ensuing exponent for the dissipation term is (-.25) rather than zero.

The result just obtained may be tested by using the weaker dissipation function described in section 2 corresponding to $\chi = 2$. In this case the model dissipation scales as $\lambda^{4-3\rho}$ in $d = 1$. If $\rho = 4/3$, the spectral exponent becomes (-2.67), which is in the right range for the cases cited earlier using this model. Unfortunately, however, this leads to nonlinear source terms in equation (8a) which scale as a positive power of λ. It is possible that this is why these models still tended to diverge numerically. Additonally, of course, the dissipation term is not dominant.

Passing to $d = 2$, equations (8a) and (8b) imply that the scaling exponents of the nonlinear interaction terms match if $\rho = 3$. With this choice each of the nonlinear terms in equation (8a) scales as $\lambda^{-5/2}$ while those in equation (8b) scale as λ^{-3}. Remarkably, for both the cases $\chi=2$ and $\chi=4$ the β–dependent dissipation term scales as λ^{-4}, suppressed with respect to the nonlinear interaction terms. The spectral exponent is then (-6), which is not acceptable.

The alternative scenario being developed seeks to predict a value of ρ which makes the dissipation dominant. In the case $\chi = 4$ one finds that $\rho = 11/5$ leads to λ^0 scaling of the dissipative term. This value succeeds in making the dissipative term overwhelm all others. In the case $\chi = 2$, the situation becomes more complicated, as in d = 1. The dissipative term scales as λ^0 if $\rho = 5/3$. Once again this leads to nonlinear source terms in both equations (8a) and (8b) which scale as a positive power of λ, so that the dissipative term is not the dominant one.

The problems in front of us begin, then, as follows. The "principle of dominant β-dependent dissipation" has arisen as a direct result of the computations reported here for $d = 1$. If we apply this principle to $d = 2$, we are led to predict asymptotic spectral falloff of the form $|\zeta_k| \propto k^{-22/5}$. Numerical convergence is not guaranteed, but it seems likely as a consequence of the principle. This rate of spectral decay is, however, again considerably larger than what is expected, exceeding even the "old Phillips" spectrum for $d = 2$.

So suppose one attempts to tune the dissipation function in such a manner that the above principle applies yet the parameter ρ is forced to take the value 7/4 in $d = 2$, thus producing the "Toba" spectrum in wave number space. We may, in fact, leave the dissipation term aside for the moment, and observe that the choice $\rho=7/4$ leads to terms in equations (8a) and (8b) which scale as positive powers of λ, threatening stability. The largest term occurs in equation (8a) and scales as $\lambda^{+5/4}$. Notice that these powers follow directly from linear combinations of ρ and d and are entirely independent of the dissipation parameter χ.

In light of this observation, can the principle of dominant dissipation lead to a prediction for the value of χ? Once restrictions discussed in section 2 regarding the argument of the dissipation function are respected, we have afresh:

$$f(k^{7/2}\psi/\sqrt{g}\,) \rightarrow (k^7|\psi|^2/g)^{\chi/2} \rightarrow \lambda^{5\chi/4}\,(k^7|\psi|^2/g)^{\chi/2}. \qquad (10)$$

Taking into account the additional factors $\omega_k\,\psi$ that enter the full dissipation function we arrive at the condition $(5\chi - 7)/4 > 5/4$, or $\chi > 12/5$. The value $\chi = 4$ certainly satisfies this condition. We see that the dissipation function may be the dominant term without necessarily determining the value of ρ provided one is willing to entertain the existence of non-negative scaling exponents in the equations of motion. Again, though, the existence of such positive exponents may threaten numerical stability.

To summarize, it has been discovered that a principle of dissipative dominance governs the asymptotic spectral exponent obtained numerically in this work. A competing principle of similar scaling of nonlinear and dissipative processes does not lead to the observed values of the exponent. Utilizing the new principle, it is possible to predict that a spectral exponent in agreement with experiment in $d = 2$ may emerge provided that the degree of nonlinearity of the dissipation function which models wave breaking exceeds a specific lower bound. It remains to be seen whether calculations in that dimensionality comparable in scope to those performed here will remain numerically stable and bear out these predictions. We have been able to argue that there does not exist a basis for ruling out possible agreement with experiment, but it must be left for future calculations to indicate if it is in fact realized.

Acknowledgements. The author thanks Michael Banner and Mark Donelan for useful discussions and suggestions. This research was entirely funded by the Rosenstiel School of Marine and Atmospheric Science, University of Miami.

References

Al-Zanaidi, M. A. and W. H. Hui, Turbulent air flow water waves, *J. Fluid Mech. 148*, 225 , 1984.

Banner, M. L., Equilibrium spectra of wind waves, *J. Phys. Oceanogr.* ***20***, 966, 1990.

Banner, M. L. and X. Tian, On the determination of the onset of breaking for modulating surface gravity water waves, *J. Fluid Mech.* ***367***, 107 , 1998.

Belcher, S. E. and J. C. R. Hunt, Turbulent shear flow over slowly moving waves, *J. Fluid Mech.* ***251***, 109, 1993.

Belcher, S. E. and J. C. Vassilicos, Breaking waves and the equilibrium range of wind-wave spectra, *J. Fluid Mech.* ***342***, 377, 1997.

Benjamin, T. B., Shearing flow over a wavy boundary, *J. Fluid Mech.* ***6***, 161, 1959.

Cohen, J. E. and S. E. Belcher, Turbulent shear flow over fast-moving waves, *J. Fluid Mech.* ***386***, 345, 1999.

Donelan, M. A., Wind-Induced Growth and Attenuation of Laboratory Waves, *Wind-over-Wave Couplings*, edited by S. G. Sajjadi, N. H. Thomas, and J.C.R. Hunt, Clarendon Press 1999.

Donelan, M. A., and W. J. Pierson, Radar scattering and equilibrium ranges in wind-generated waves with application to scatterometry, *J. Geophys. Res.* ***92***, *C5*, 4971, 1987.

Dyachenko, A. I. and V. E. Zakharov, Is free-surface hydrodynamics an integrable system?, *Physica D 87 (1-4)*, 233, 1995.

Hara, T. and C. C. Mei, Frequency downshift in narrowbanded surface-waves under the influence of wind, *J. Fluid Mech.* ***230***, 429, 1991.

Jeffreys, H., On the formation of waves by wind, *Proc. Roy. Soc., London, Ser.* ***A, 107***, 189, 1924.

Jeffreys, H., On the formation of waves by wind II, *Proc. Roy. Soc., London, Ser.* ***A, 110***, 341, 1925.

Kitaigorodskii, S. A., On the theory of the equilibrium range in the spectrum of wind-generated gravity waves, *J. Phys. Oceanogr.* ***13***, 816, 1983.

Komen, G. J., S. Hasselmann, and K. Hasselmann, On the existence of a fully developed wind-sea spectrum, *J. Phys. Oceanogr.* ***14***, 1271, 1984.

Komen, G. J., et al. *Dynamics and Modelling of Ocean Waves*, 532 pp., Cambridge Univ., New York, 1994.

Krasitskii, V. P., On reduced equations in the Hamiltonian theory of weakly nonlinear surface waves, *J. Fluid Mech.* ***272***, 1,1994.

Landau, L. and E. M. Lifshitz, *Mechanics*, Addison-Wesley, New York, 1960.

Magnusson, A. K., M.A. Donelan and W.M. Drennan, On estimating extremes in an evolving wave field, *Coastal Eng.*, ***36***, 147, 1999.

Phillips, O.M., Spectral and statistical properties of the equilibrium range in wind-generated gravity waves, *J. Fluid Mech.* ***156***, 156, 1985.

Pierson, W. J., *Surface Waves and Fluxes*, vol. 2, edited by G. L. Geernaert and W. L. Plant, Kluwer Acad., Norwell, Mass., 1990.

Pierson, W. J. and L. Moskowitz, A proposed spectral form for fully developed wind seas based on the similarity theory of S. A. Kitaigorodskii, *J. Geophys. Res.* ***69***, 5181, 1964.

Plant, W. J., A relation between wind stress and wave slope, *J. Geophys. Res.* ***C87***, 1961, 1982.

Pushkarev, A. N., and V. E. Zakharov, Turbulence of capilliary waves, *Phys. Rev. Lett.*, ***76(18)***, 3320, 1996.

Pushkarev, A.N., and V. E. Zakharov, Turbulence of capilliary waves-Theory and numerical simulation, *Physica D* ***135***, 98, 2000.

Smith, R. A., An operator expansion formalism for nonlinear surface waves over variable depth, *J. Fluid Mech.* ***363***, 333, 1998.

Watson, K. M. and S. B. Buchsbaum, Interaction of capillary waves with longer waves. 1. General theory and specific applications to waves in one dimension, *J. Fluid Mech.* ***321***, 87, 1996.

West, B. J., A resonant test-field model of gravity waves, *J. Fluid Mech.* ***132***, 417, 1983.

Willemsen, J. F., Analysis of SWADE Discus N wind speed and wave height time series, part II, Quantitative growth rates during a storm. *J. Oceanic Atmos.Technol.* ***14***, 630, 1997.

Willemsen, J. F., Enhanced Computational Methods for Nonlinear Hamiltonian Wave Dynamics, *J. Oceanic Atmos.Technol.*, ***15***, 1517, 1998.

Willemsen, J.F., Enhanced Computational Methods for Nonlinear Hamiltonian Wave Dynamics, part II, New results, *J. Oceanic Atmos.Technol. 18*, 775, 2001.

Zakharov, V., and N. N. Filonenko, The energy spectrum for stochastic oscillations of a fluid surface, *Dokl. Akad. Nauk SSSR*, ***170(6)***, 1292, 1966.

J. F. Willemsen, Rosenstiel School of Marine and Atmospheric Science, University of Miami, 4600 Rickenbacker Causeway, Miami, FL 33149. (jorge@maya.rsmas.miami.edu)

(Received March 30, 2000; revised February 20, 2001; accepted May 21, 2001.)